Microsoft® Research
WorldWide Telescope

Experience WWT at **worldwidetelescope.org**

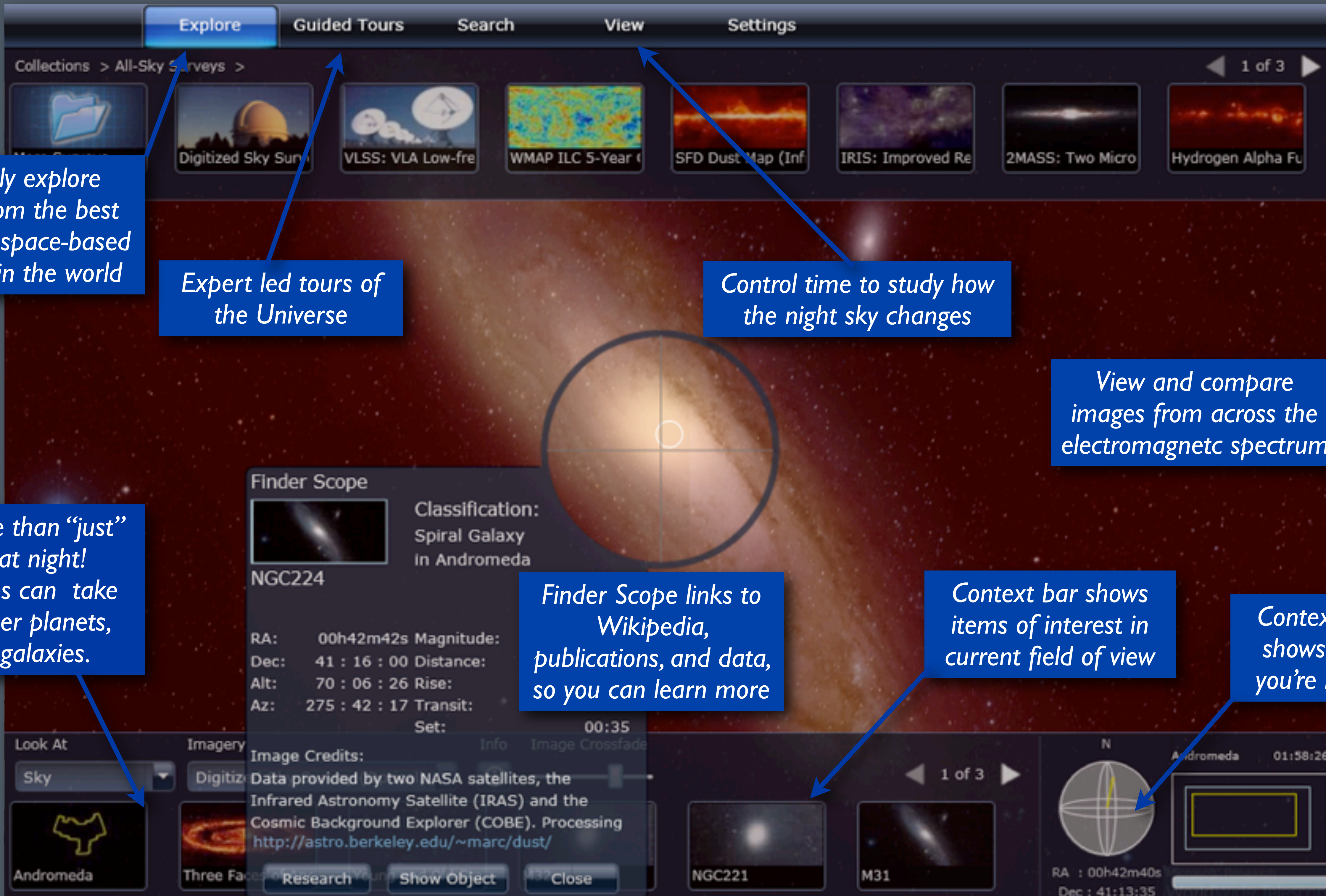

Avatar, Another Talk, or Both?

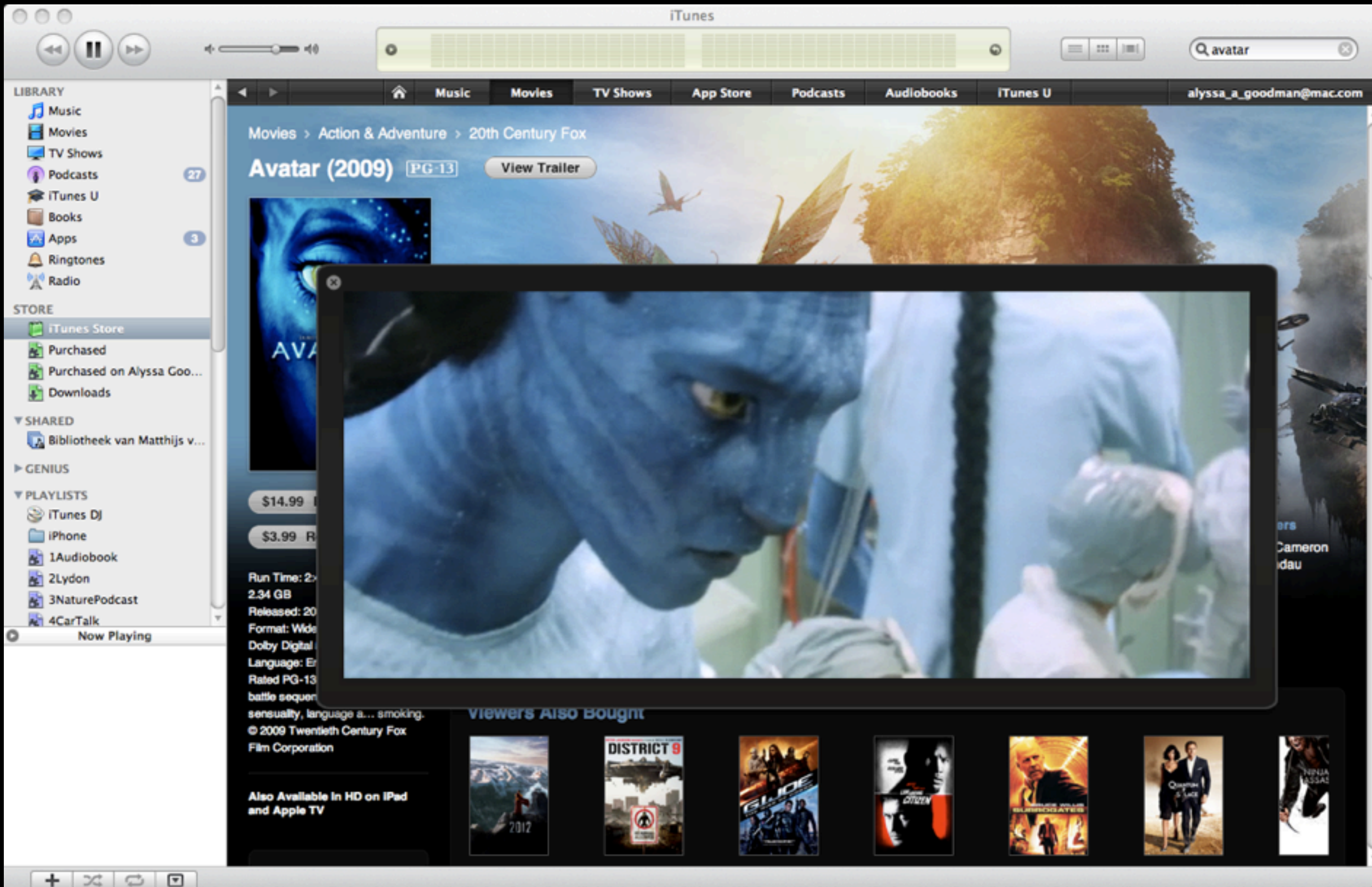

Comparisons between Simulations and Observations… Where we Stand

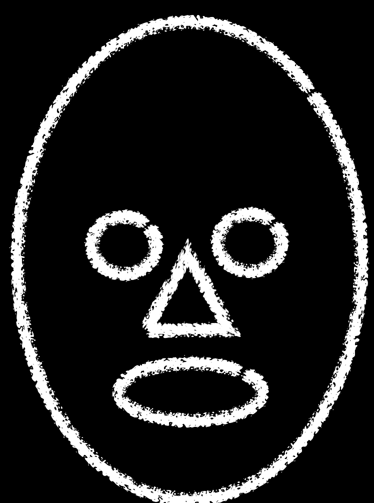

Alyssa A. Goodman (et al.!)
Harvard-Smithsonian Center for Astrophysics

What can be done, where, and how?

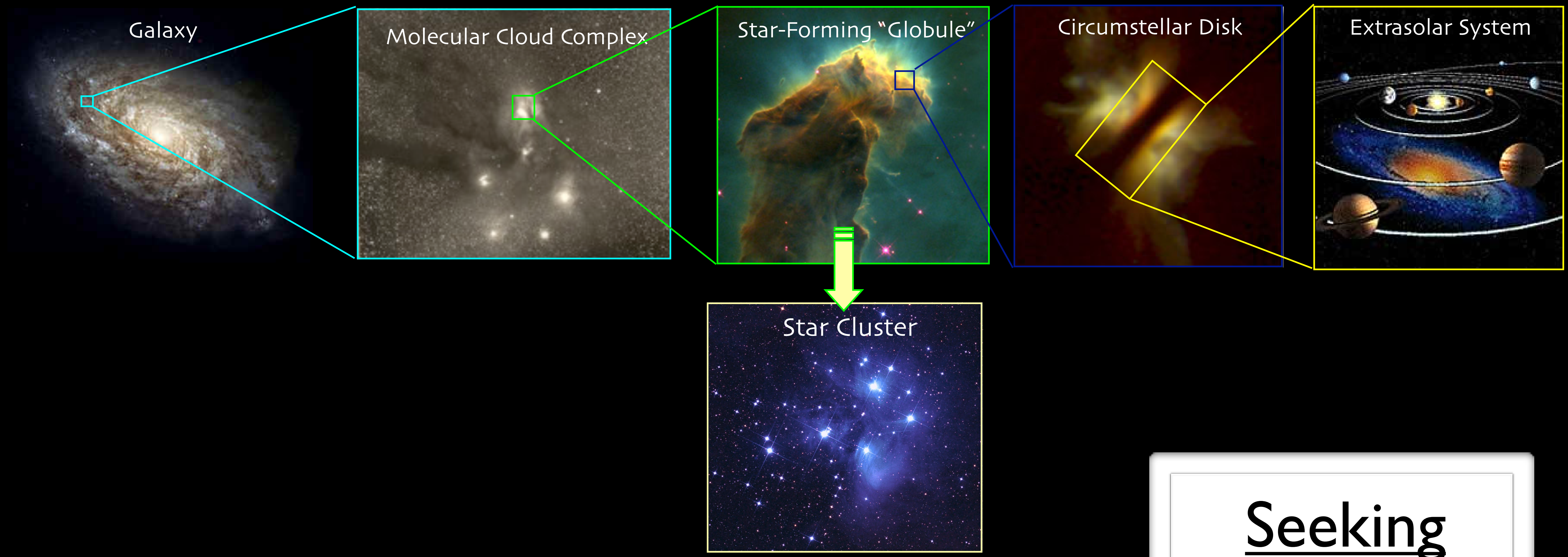

<u>Seeking</u>

n, *T*, ***v***, *X*..., ***B***

of (***x***,*t*)

"UNRESOLVED" measures

Integrated Intensity Ratios(gas, dust) 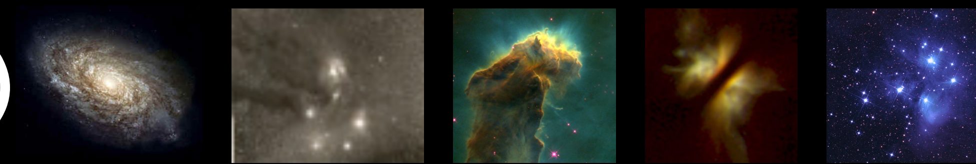

counting statistics 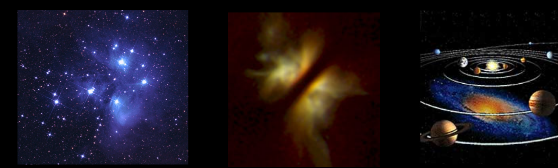

★ SED modeling 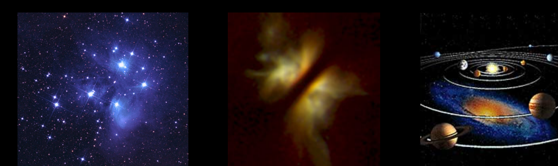

<u>Seeking</u>

$n, T, \mathbf{v}, X..., \mathbf{B}$

of $(\mathbf{x}, t)$

"RESOLVED" measures

★ Dust: Extinction 

★ Dust: Emission 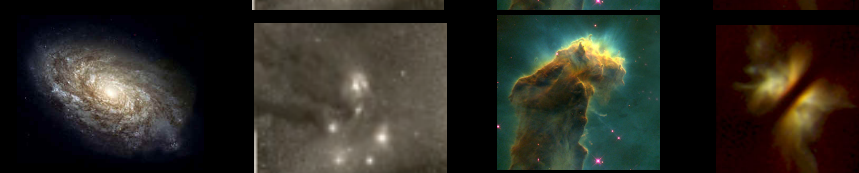

★ Dust: Scattered light 

★ Dust/gas: Polarization (abs/scatt/em) 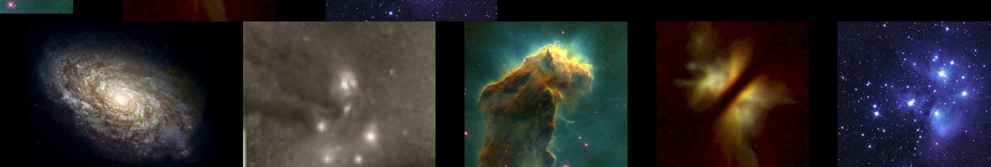

Gas: Zeeman (abs/em) 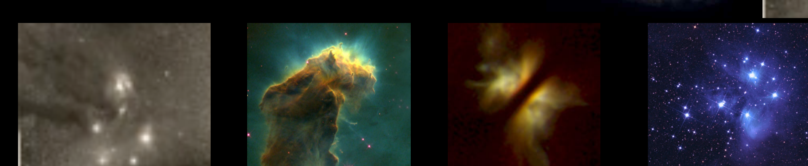

★ Gas: Detailed *p-p(-v)* maps/analysis 

"UNRESOLVED" measures

- ★ SED modeling  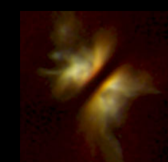 

"RESOLVED" measures

- ★ Dust: Extinction    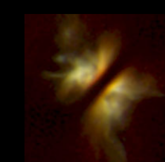
- ★ Dust: Emission    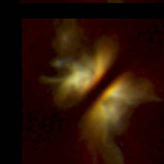
- ★ Dust: Scattered light   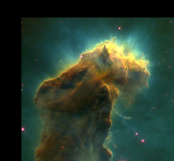 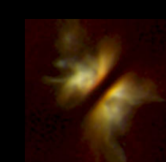 
- ★ Dust/gas: Polarization (abs/scatt/em)  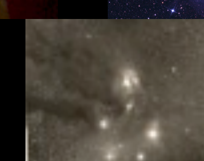  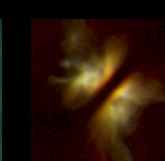 
- ★ Gas: Detailed *p-p(-v)* maps/analysis    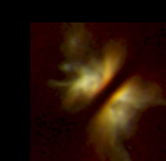

"Review" will note the work of...

Galaxy Scale

Rosolowsky et al.

Dobbs et al.

GMC Scale

Lazarian, Pogosyan, et al.

Heyer, Brunt et al.

E. Ostriker, Stone & Gammie

HII Regions

Jane Arthur et al. (HII regions)...

Clouds/Cores

Rosolowsky et al.

Padoan et al.

Juvela et al.

R. Smith, Bonnell et al.

H. Kirk et al. (including S. Basu)

Cores/Disks

Offner, Krumholz, et al.

Schnee, Kauffmann, Shetty et al.

Steinacker et al.

J. Foster et al.

J.E. Pineda et al.

Cores/Clusters

Rundle, Harries, Acreman, Bate

Ayliffe, Bate et al.

Sources

Robitaille et al.

Whitney et al.

...and surely several others!

The “Real” M17

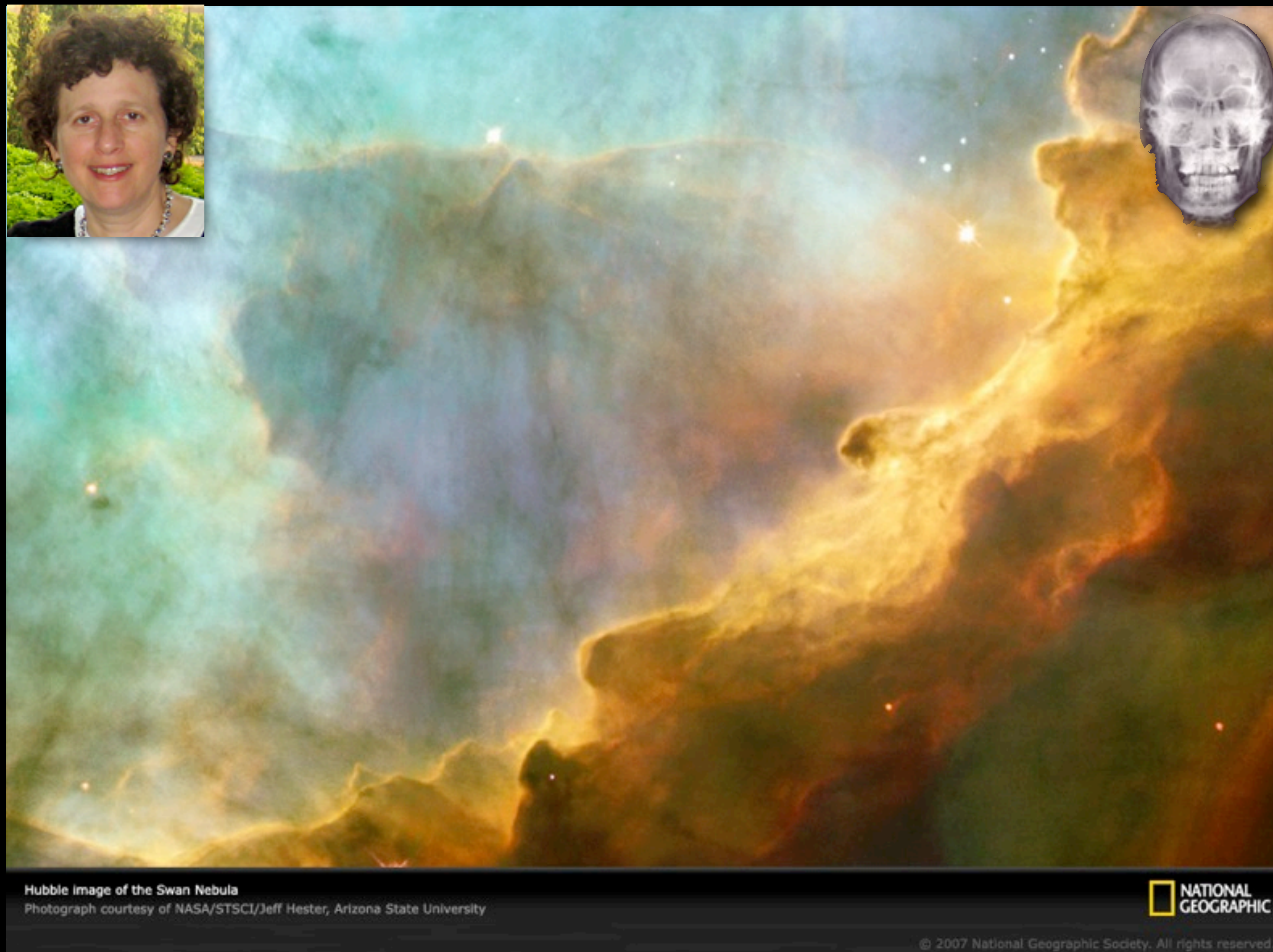

HST [OIII], Hα and [NII] emission-line image from Hester et al.

FANTASTIC! Now we need to "Taste" it...

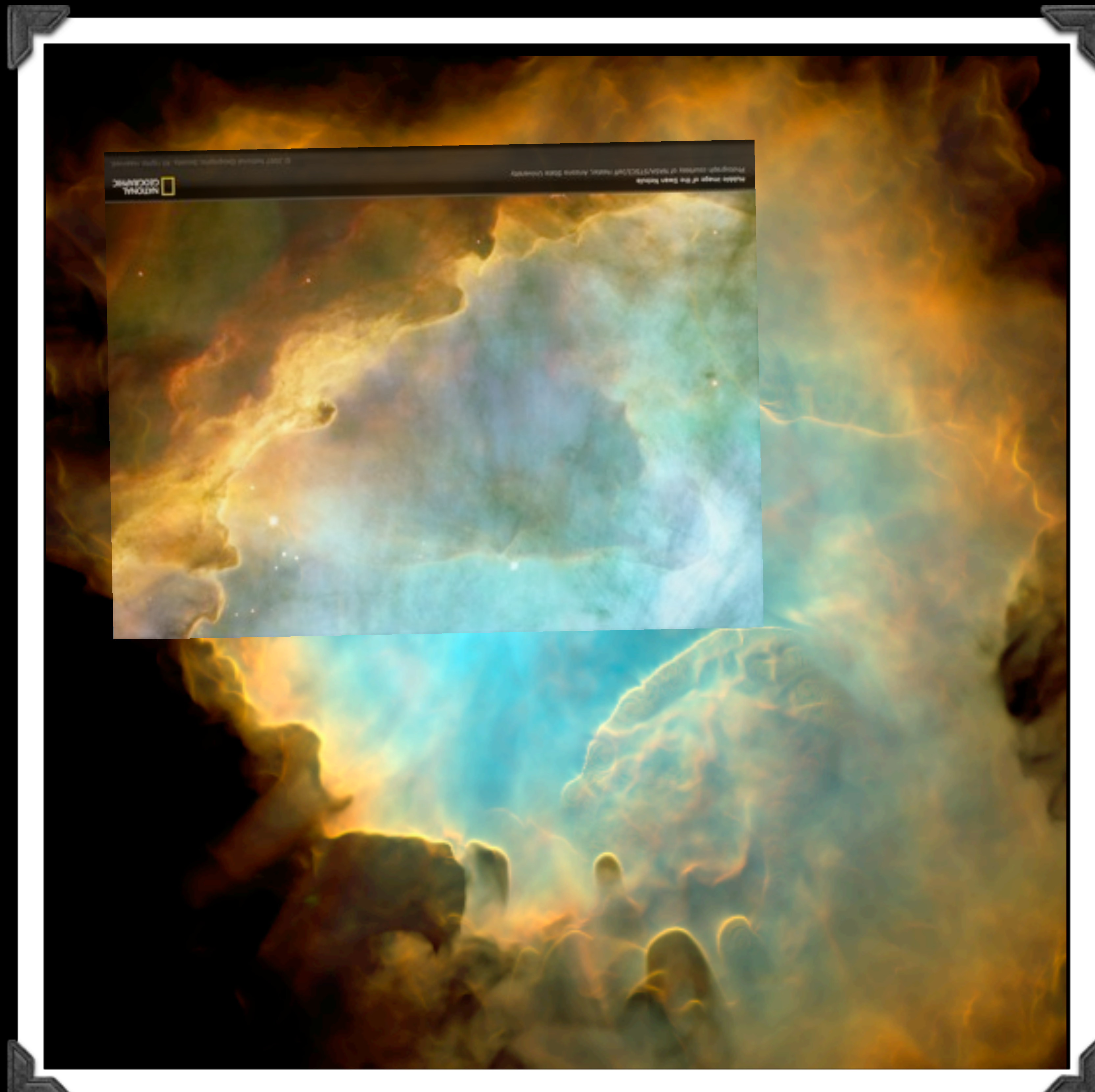

*Synthetic [OIII], Hα and [NII] emission-line image from a 512^3 numerical simulation: Mellema, Henney, **Arthur** & **Vàzquez-Semadeni** 2009*

What is "Taste-Testing"?

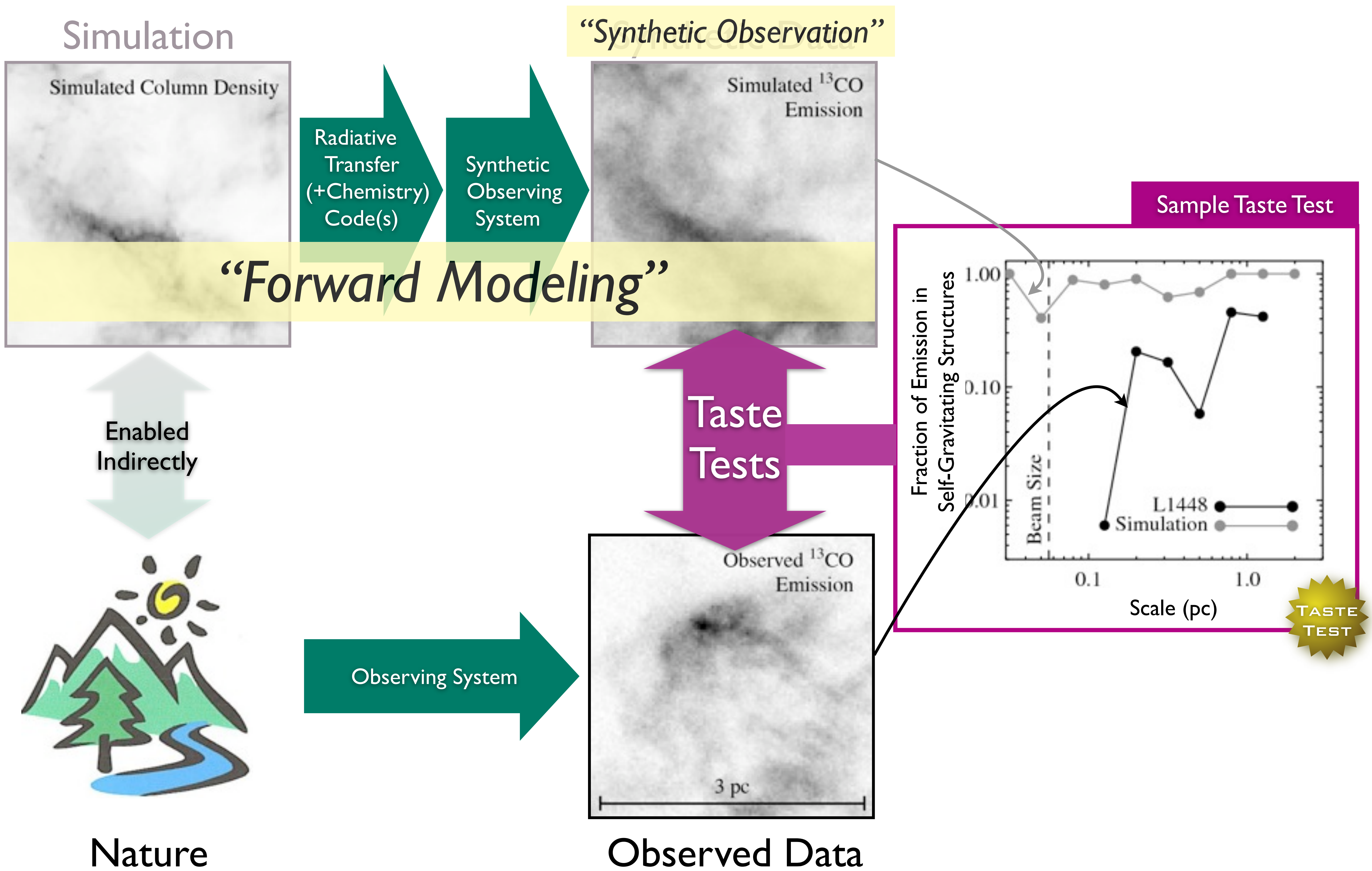

Dust: Polarimetry

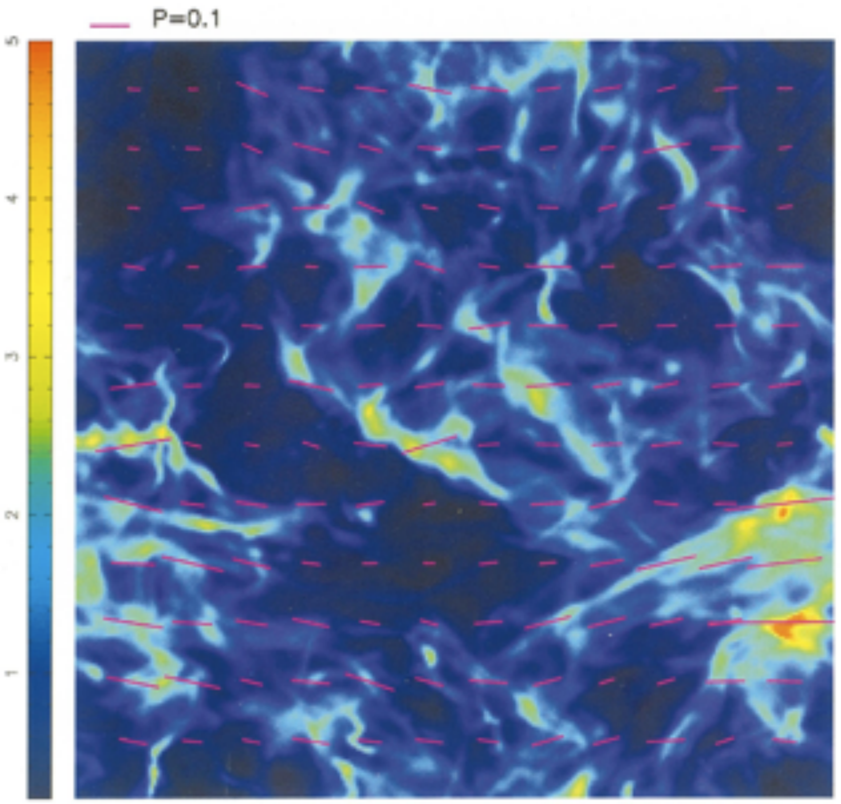

FIG. 22.—Column density (*color scale, with units* $\bar{\rho}L$) and simulated polarization map for model snapshot B2 ($\beta = 0.01$, $\mathcal{M} = 7$), projected along $\hat{z}$ perpendicular to the mean magnetic field. The fractional polarization at each point is proportional to the value of a fiducial polarization P corresponding to a uniform medium and uniform magnetic field perpendicular to the line of sight, arbitrarily set here to $P = 0.1$ as shown in the key.

Synthetic Optical Polarization Map;
Ostriker, Stone & Gammie 2001

See Ram Rao's talk....

TASTE TEST

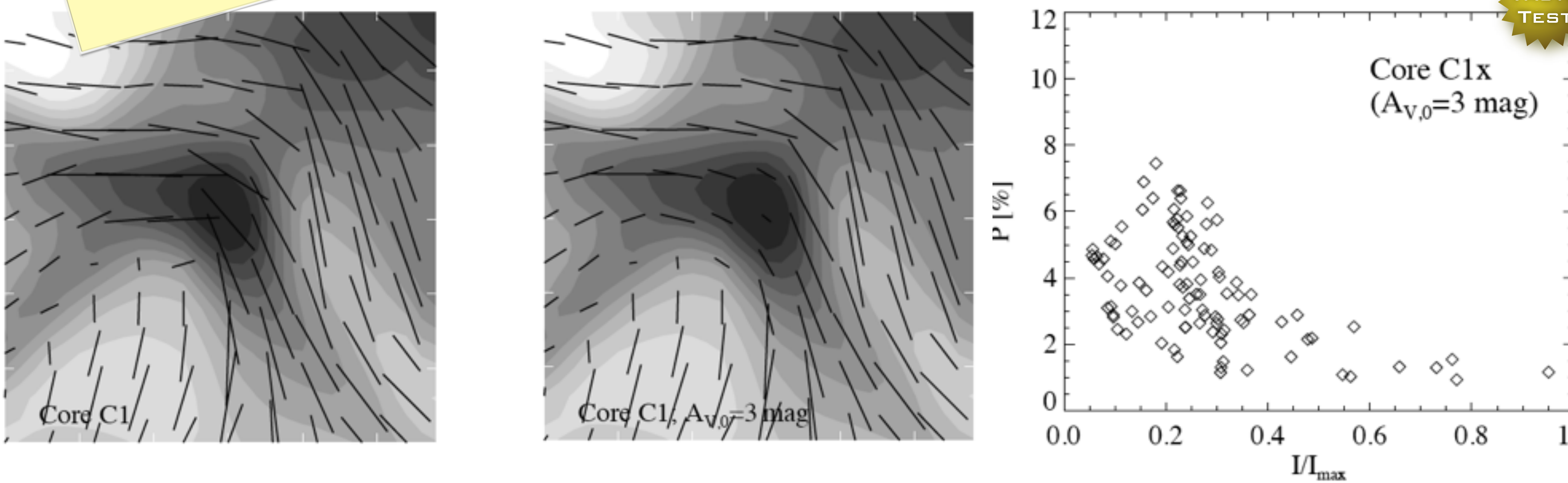

Sub-mm "Polarization Holes" caused by poorly aligned grains; *Padoan et al. 2001*

Dust: Scattered light

...can give **exquisite resolution column density maps**

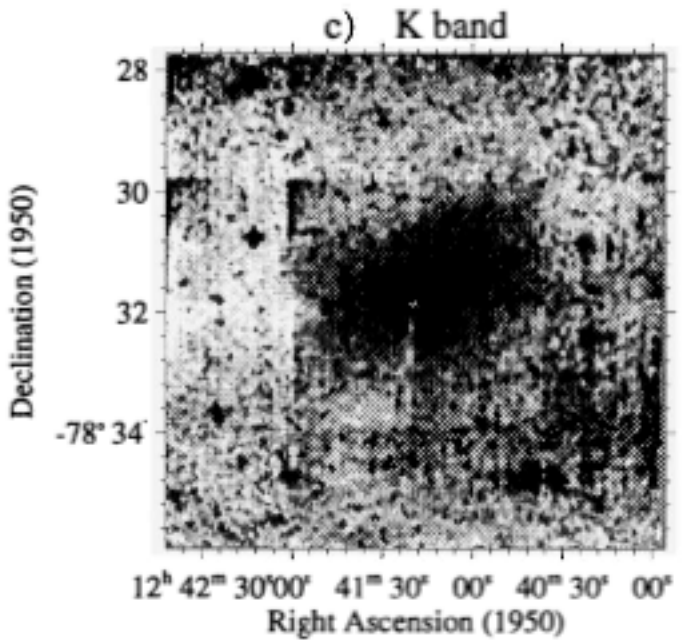

First NIR Detection; *Lehtinen & Mattila 1996*

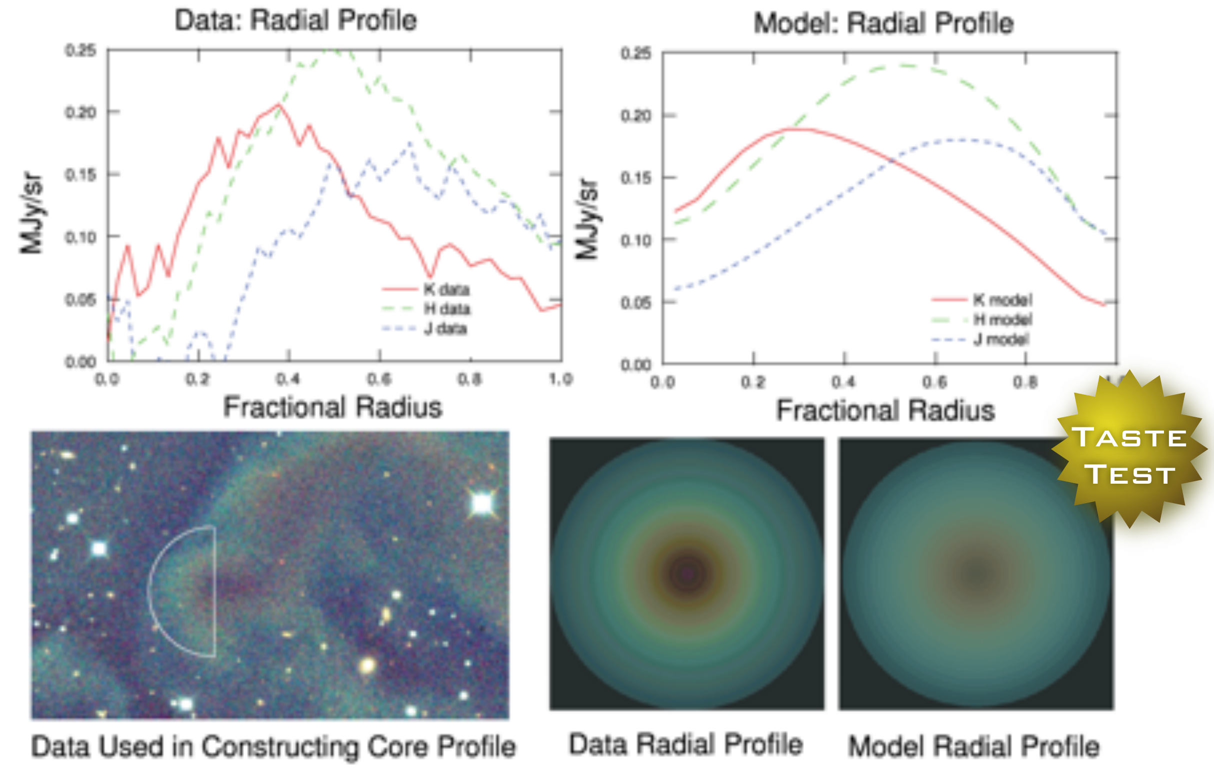

NIR "Cloudshine"; *Foster & Goodman 2006*

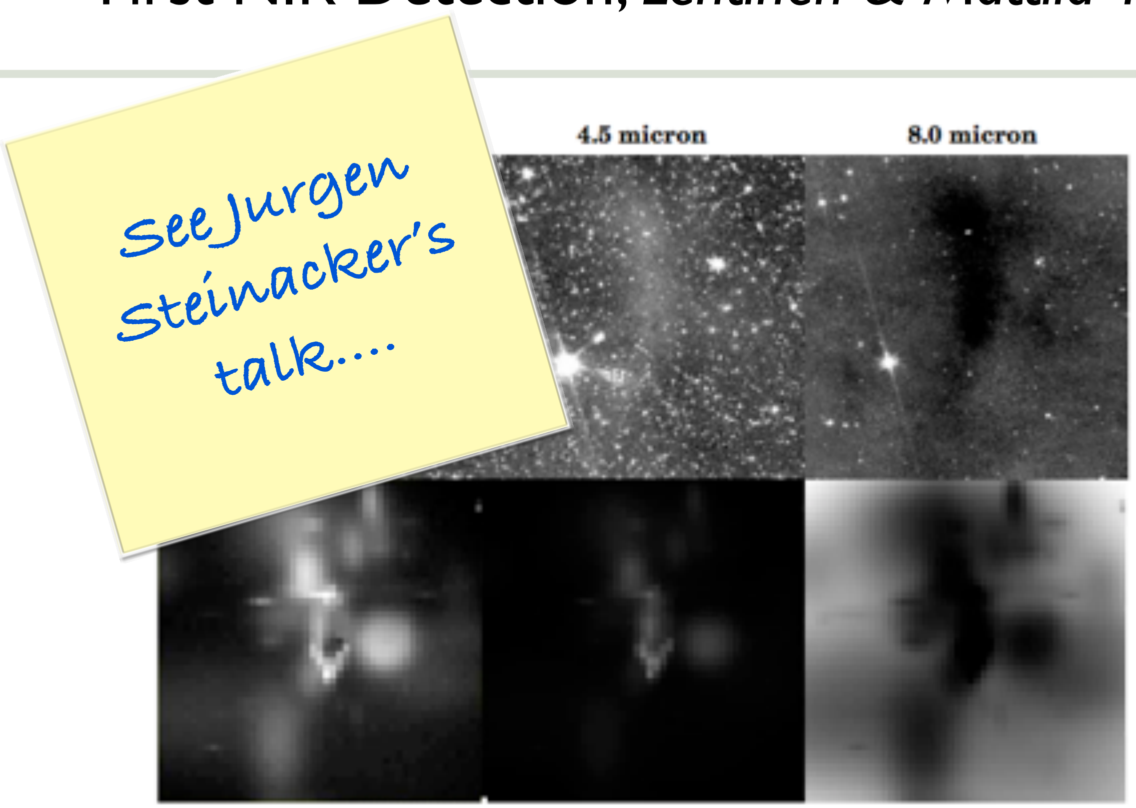

Fig. 8. Comparison of the three Spitzer images at 3.6, 4.5, and 8 μm of the inner 66000 AU of L183 (top) with scattered light models based on grains growing as a function of density (bottom). The underlying 3D structure of the model images is consistent with the measured A_V map. The general pattern of the modeled diffuse emission is similiar while, the flux is about a factor of 2 lower in the model.

MIR "Coreshine"; *Steinacker et al. 2010*

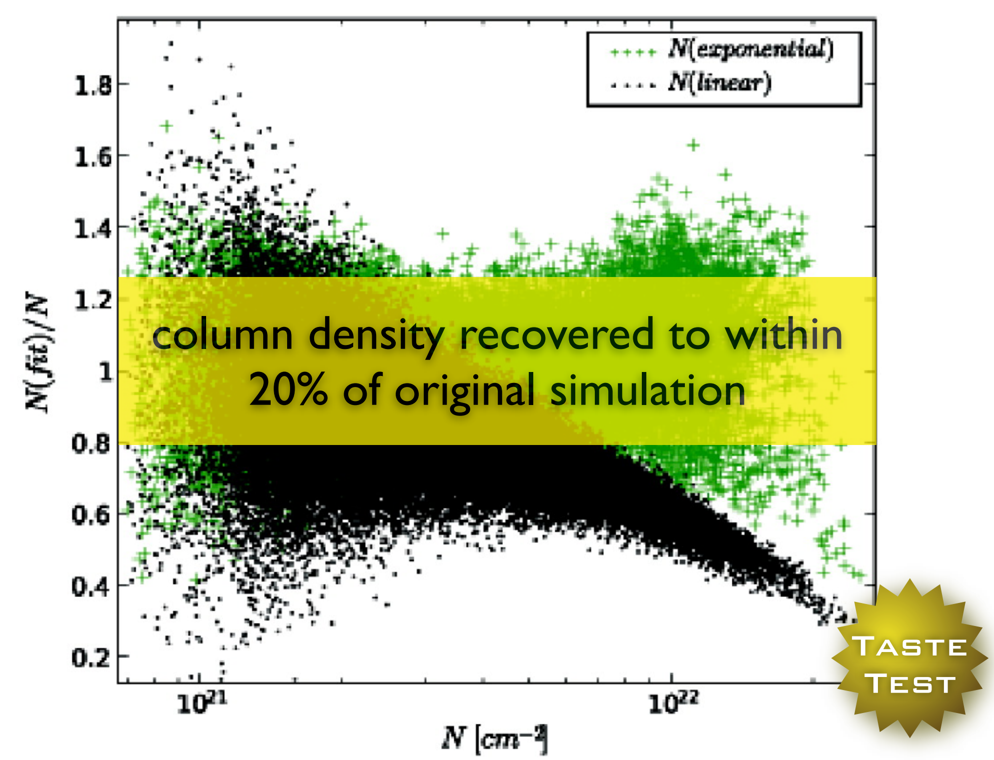

"Inversion" of Cloudshine: *Padoan, Juvela & Pelkonen 2006; Juvela, Pelkonen, Padoan, Mattila 2006*

“Cloudshine”

*(note this image is used to measure **extinction** too!)*

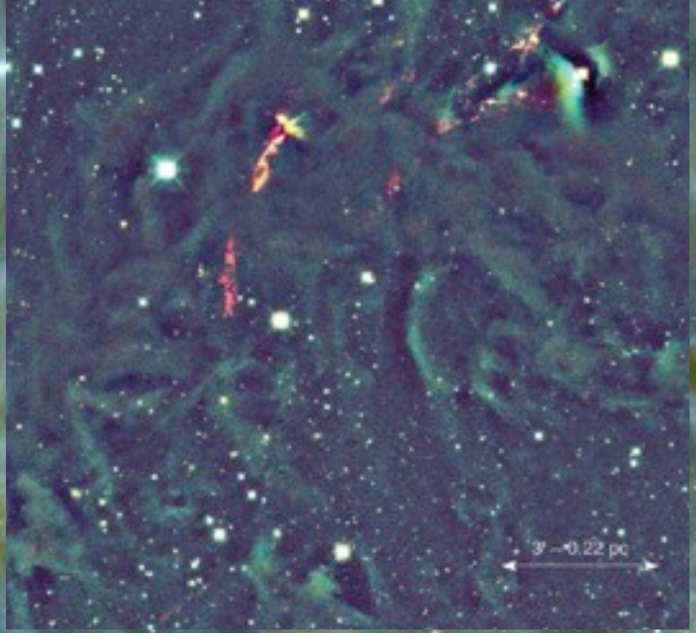

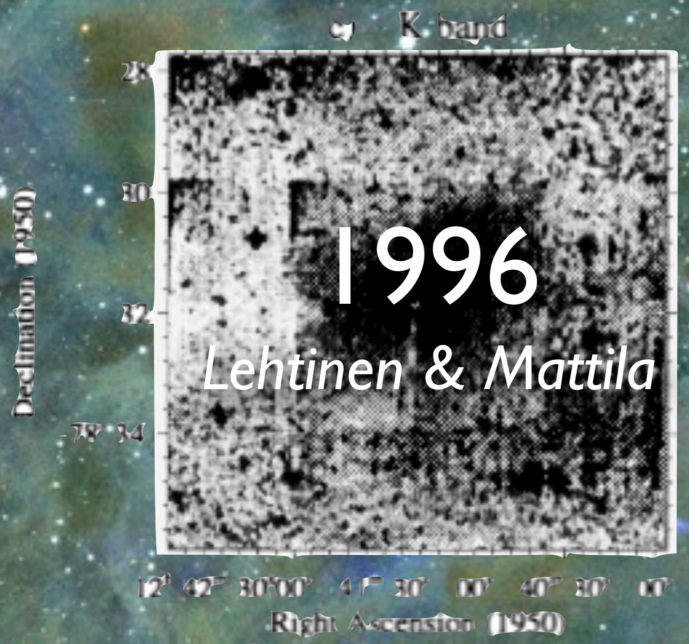

1996

Lehtinen & Mattila

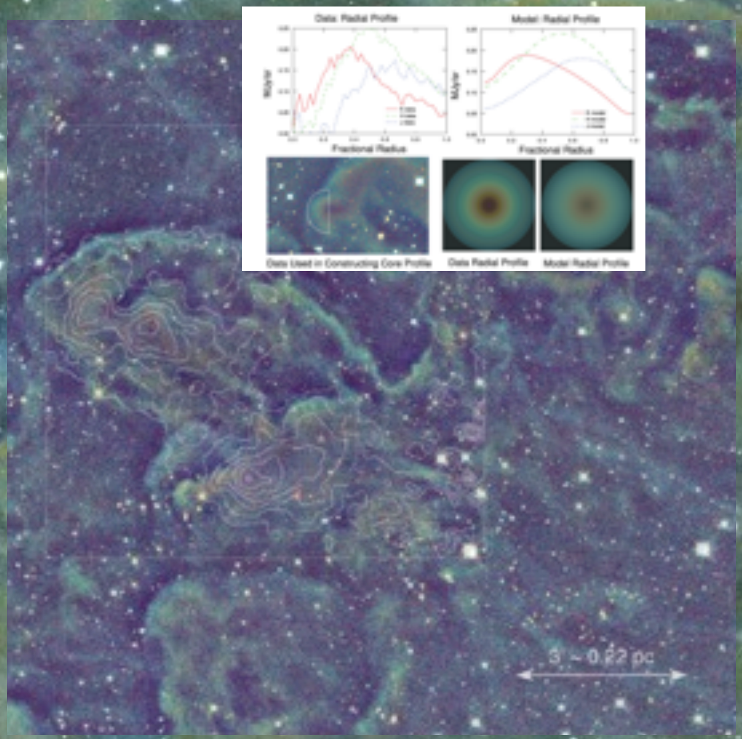

Background: to appear in Foster, Mandel, Pineda, Covey & Goodman 2010

Insets: Foster & Goodman 2006, Calar Alto JHK

Dust: Emission

Not enough time for proper discussion, but ask a question about Herschel...

See also Mika Juvela's talk, and poster by J. Malinen et al.

Orion Core Shapes from AMR Simulations (Offner & Krumholz 2009)

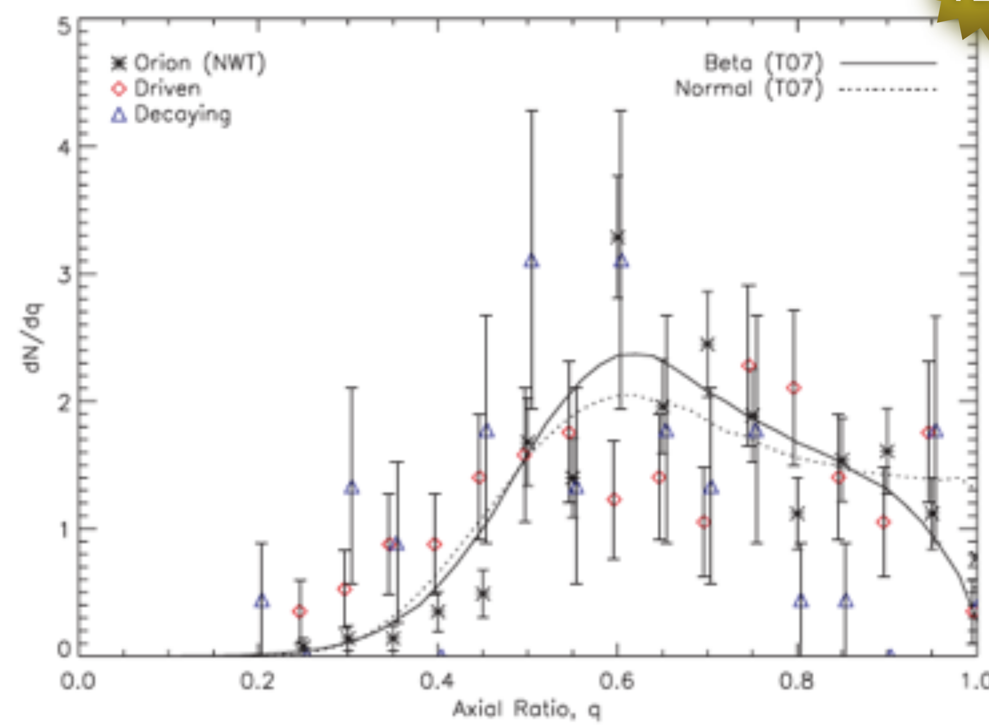

Even the "Column Temperature" is much more uncertain than you would think (even for Herschel)
Shetty, Kauffmann, Schnee, Goodman, Ercolano 2009

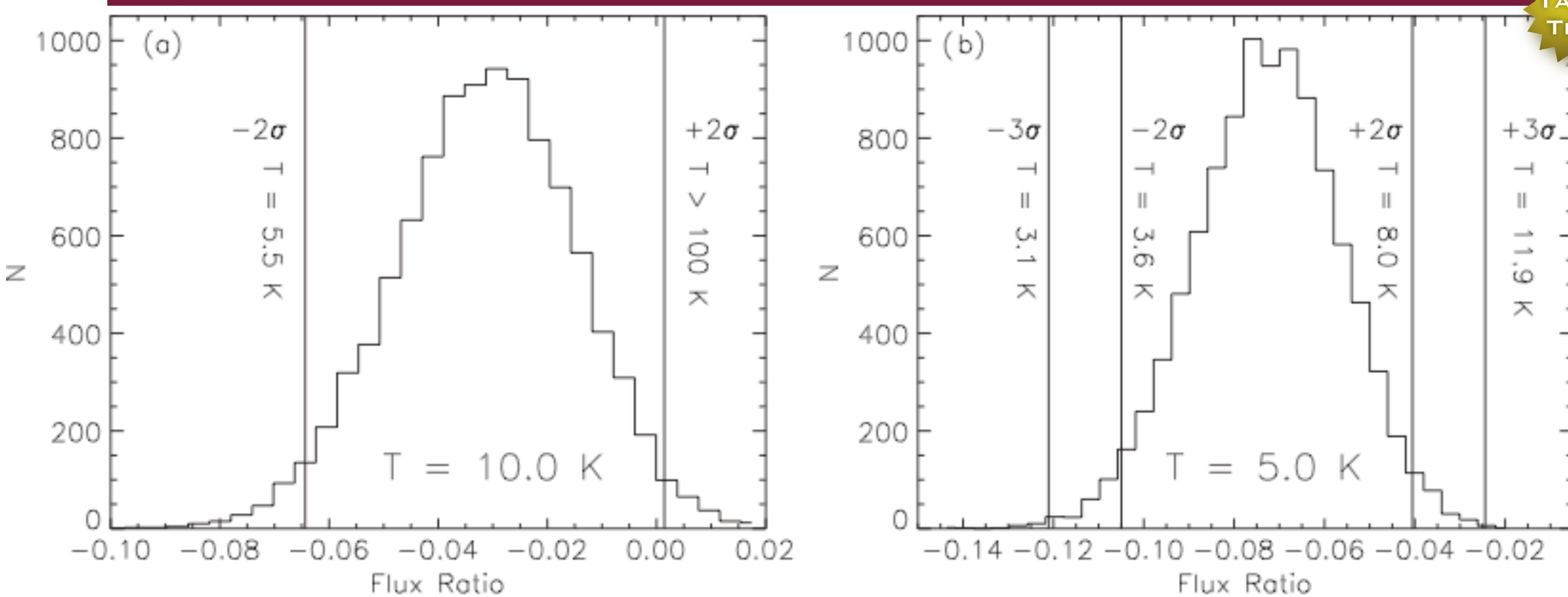

Gas: Detailed *p-p(-v)* maps/analysis

Small Stellar and Core-to-Environment **Velocities**
Offner, Hansen & Krumholz 2009; cf. Ayliffe et al. 2007; Rundle et al. 2010; Kirk et al. 2010

Taste Test

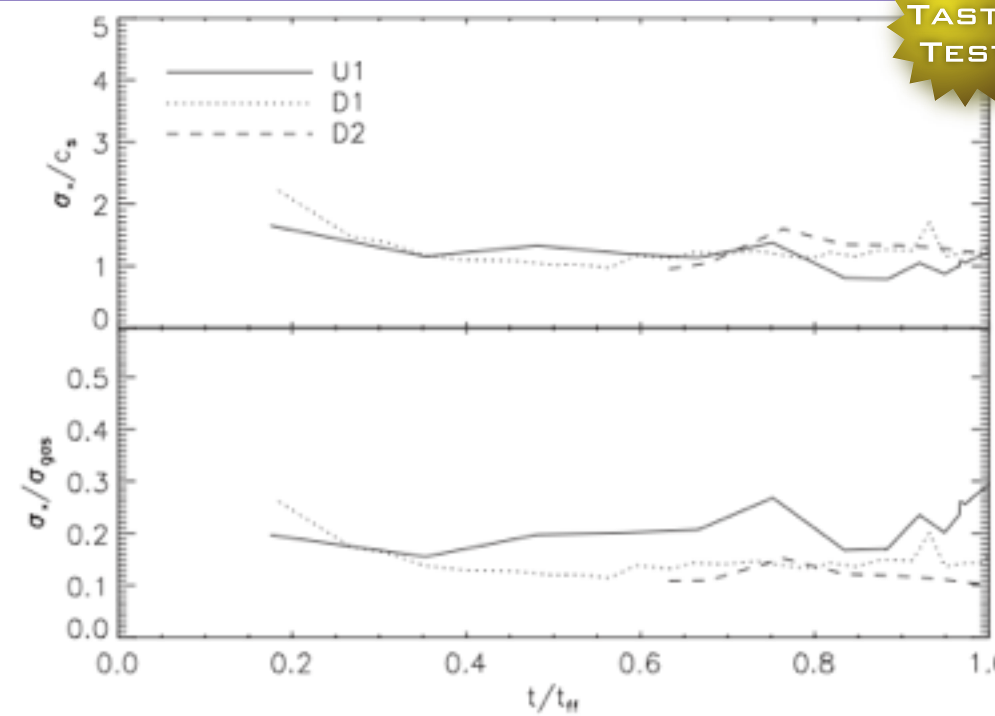

The Spectral Correlation Function
Need for High Mach Numbers...
Padoan et al. 2003;
cf. Rosolowsky et al. 1999, etc.

Taste Test

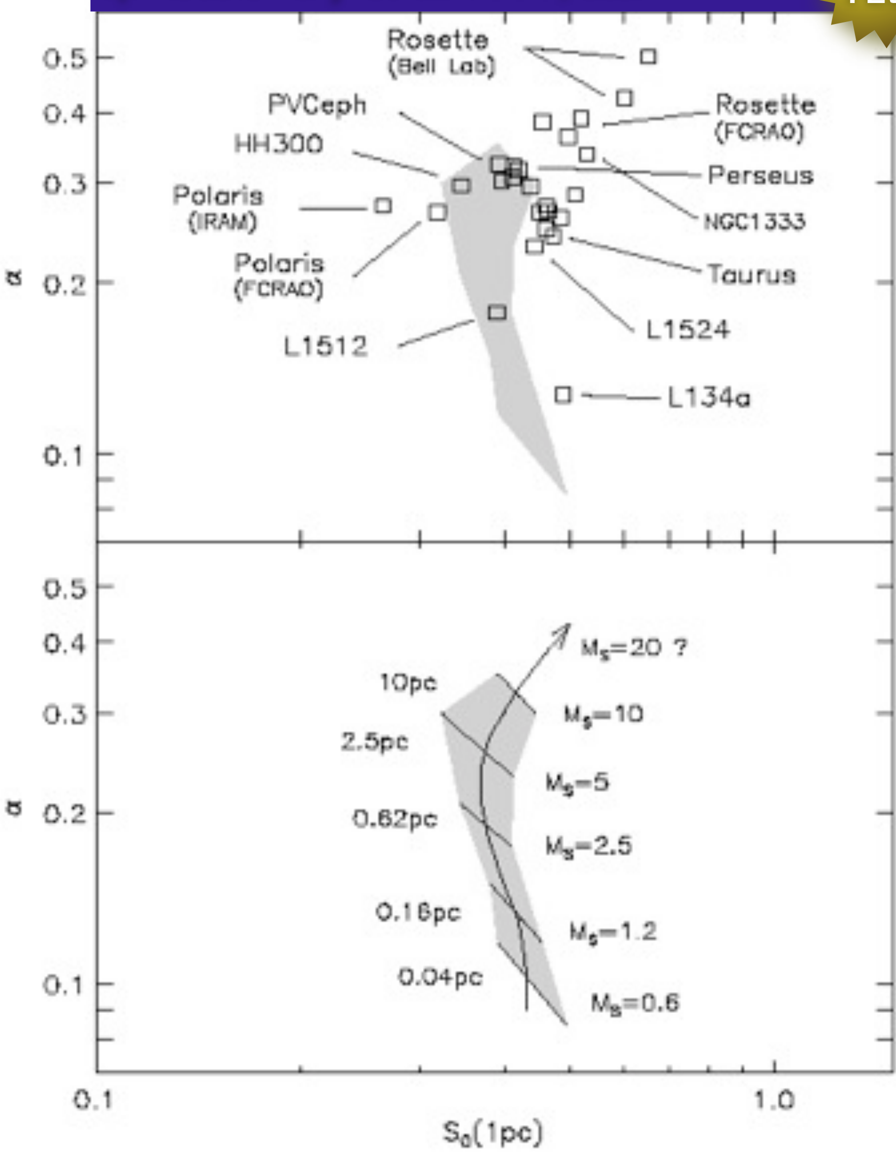

"The Perils of CLUMPFIND" – **Any CMF you want?!**
Pineda, Rosolowsky & Goodman 2009

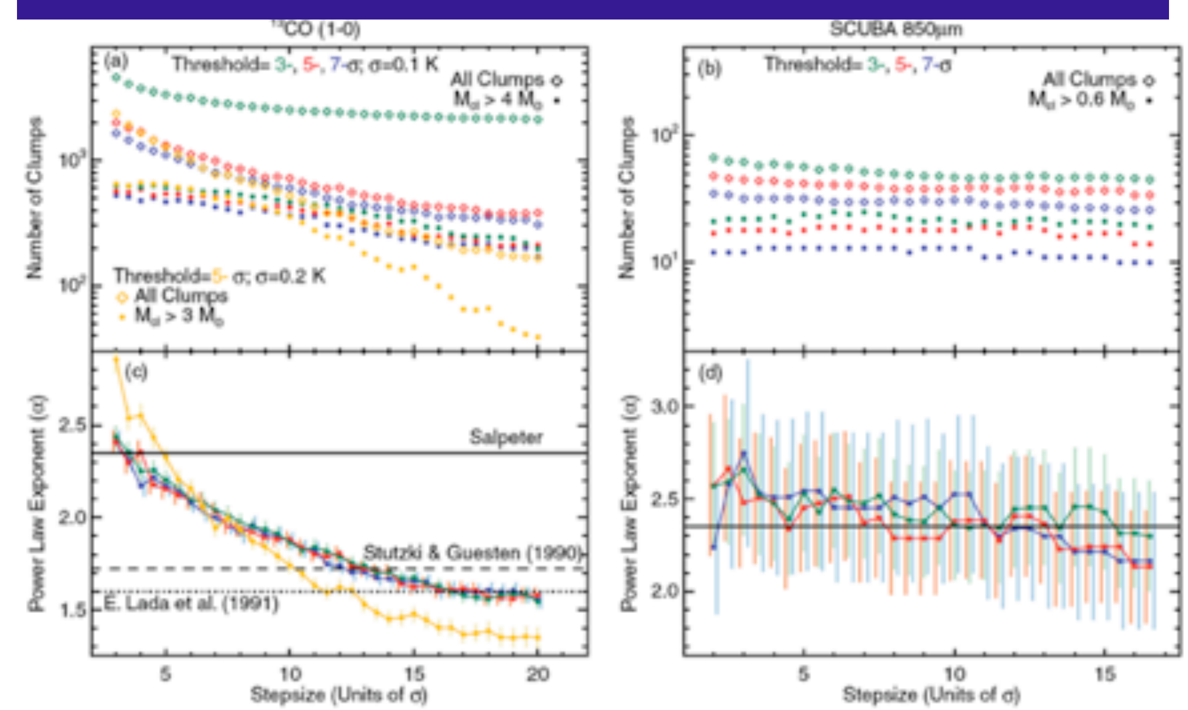

COMPLETE Perseus

- mm peak (Enoch et al. 2006)
- sub-mm peak (Hatchell et al. 2005, Kirk et al. 2006)
- ^{13}CO (Ridge et al. 2006)
- mid-IR IRAC composite from c2d data (Foster, Laakso, Ridge, et al. in prep.)
- Optical image (Barnard 1927)

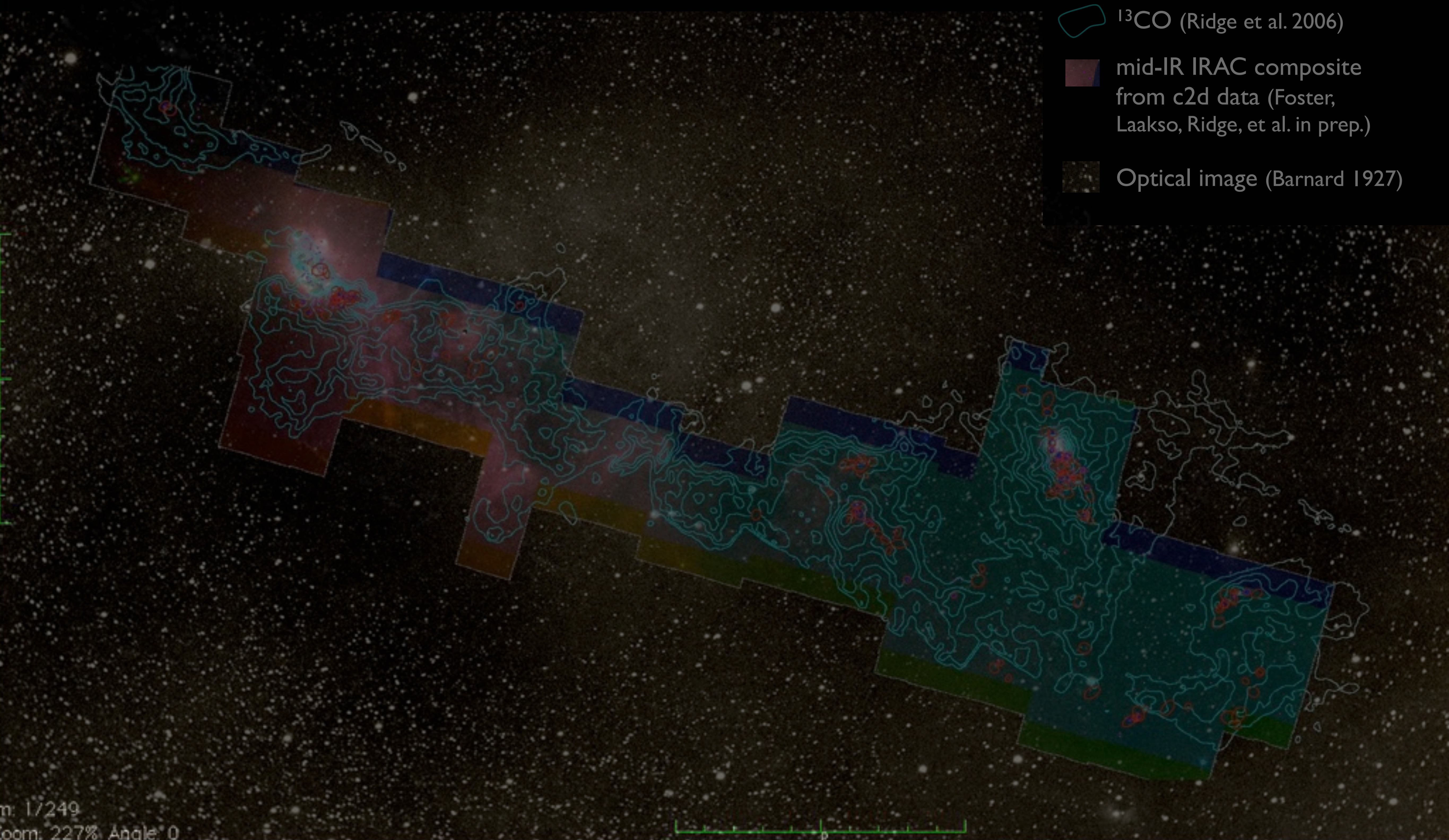

"p-p-v" NOT p-p-p (,v-v-v)

"KEITH"	"PERSEUS"
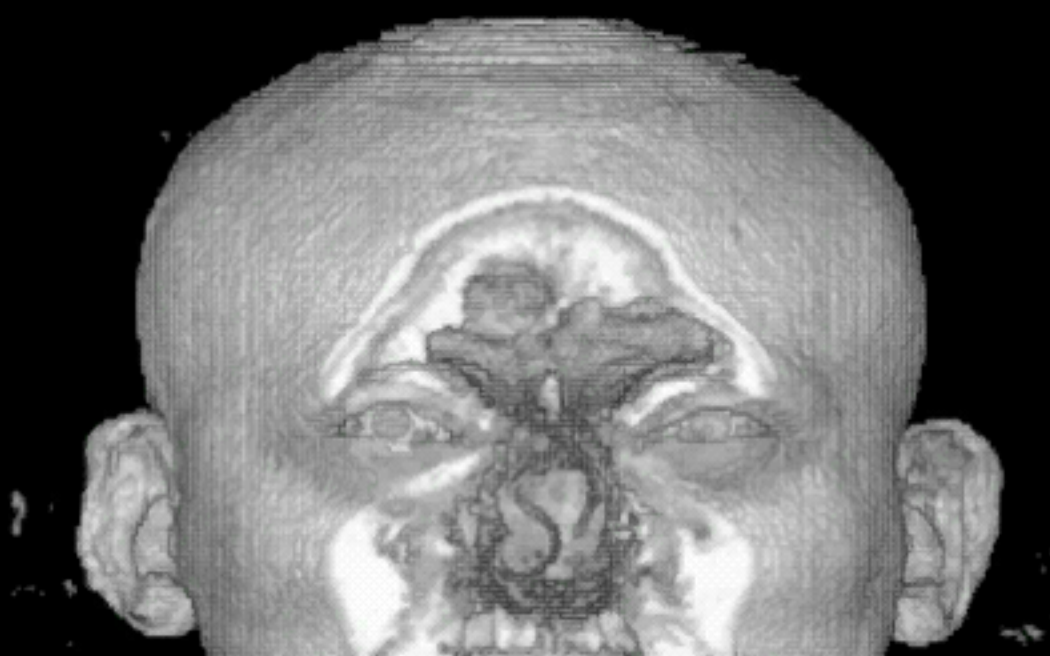	
"z" is depth into head	"z" is line-of-sight velocity

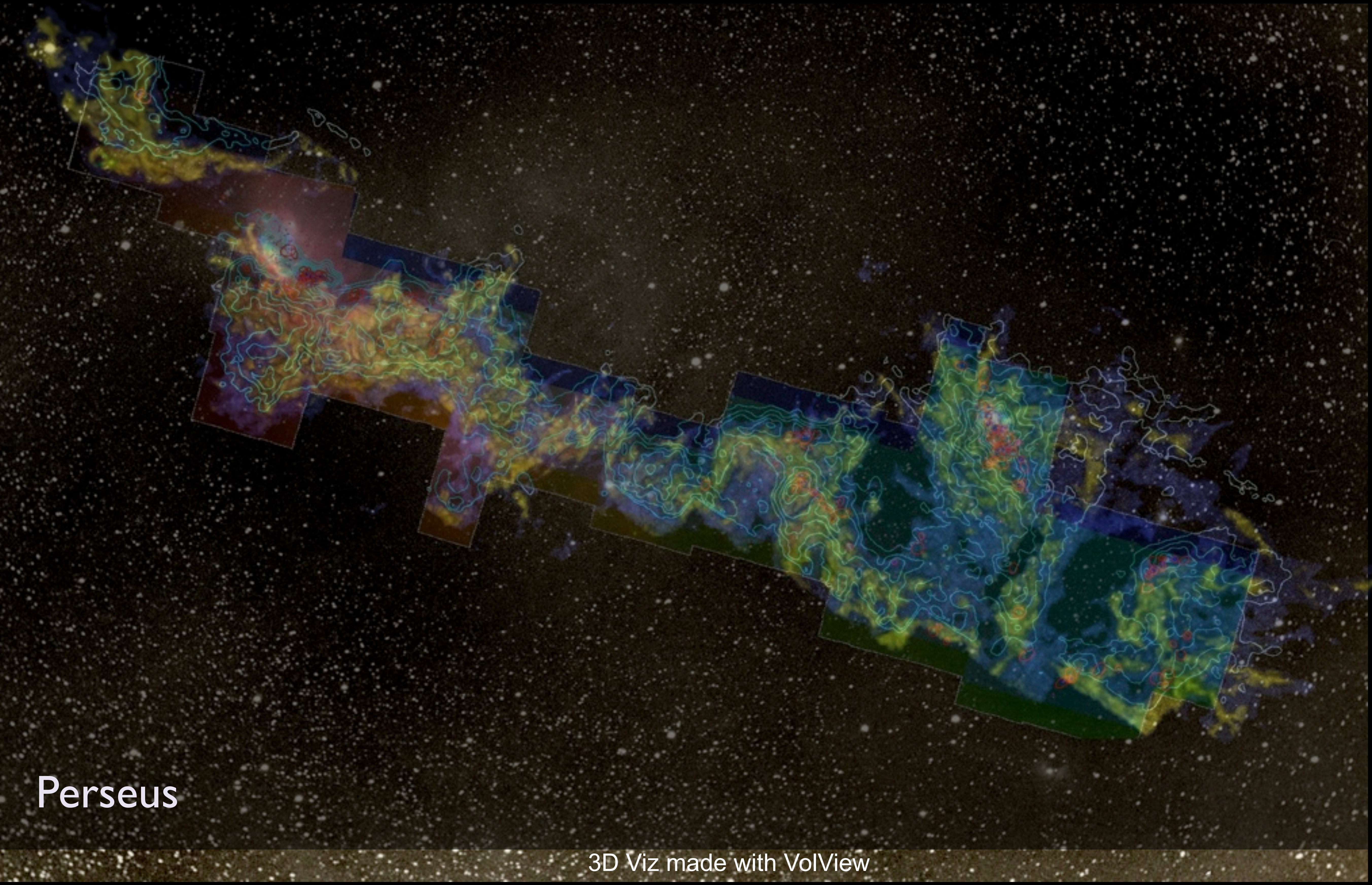
Perseus
3D Viz made with VolView

Taste-Test in p-p-v

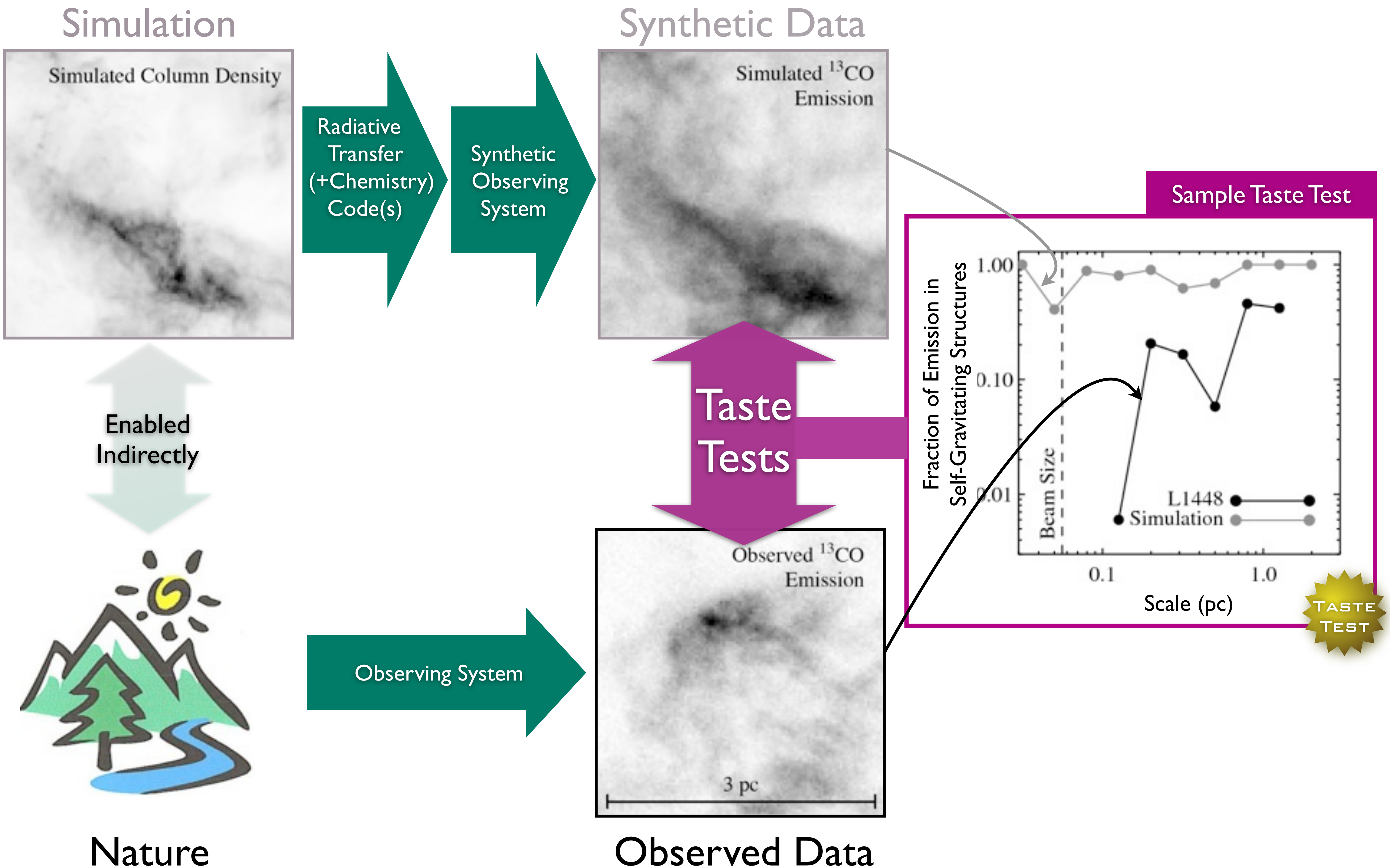

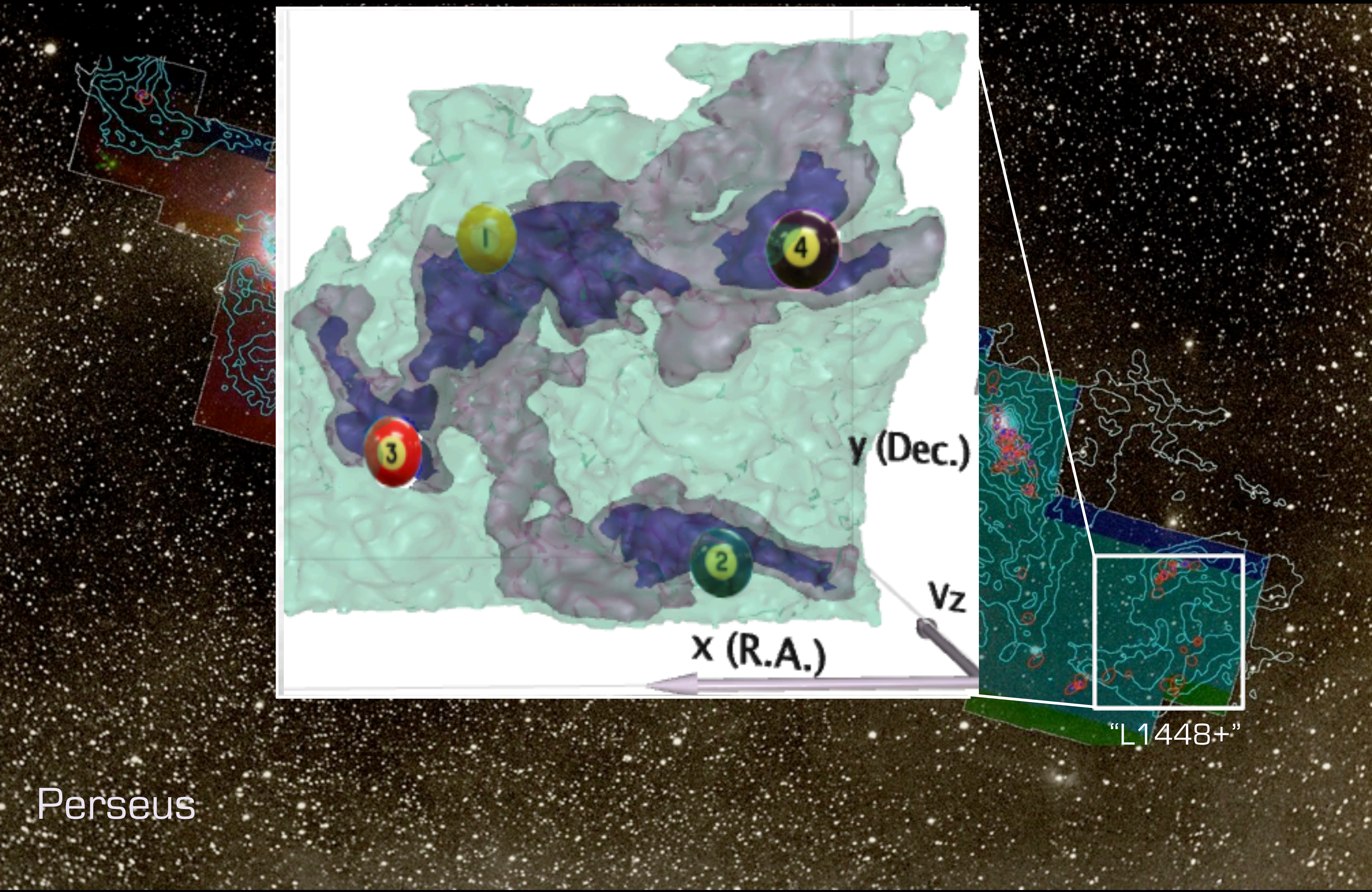

COMPLETE

Conclusion

Dendrogram-based analysis shows that **star formation takes place in self-gravitating “cocoons,”** and **some** of those **cocoons are likely bound to each other**.

But, that’s not today’s point...

Let’s see how the Taste Test Works, using 3D PDF...

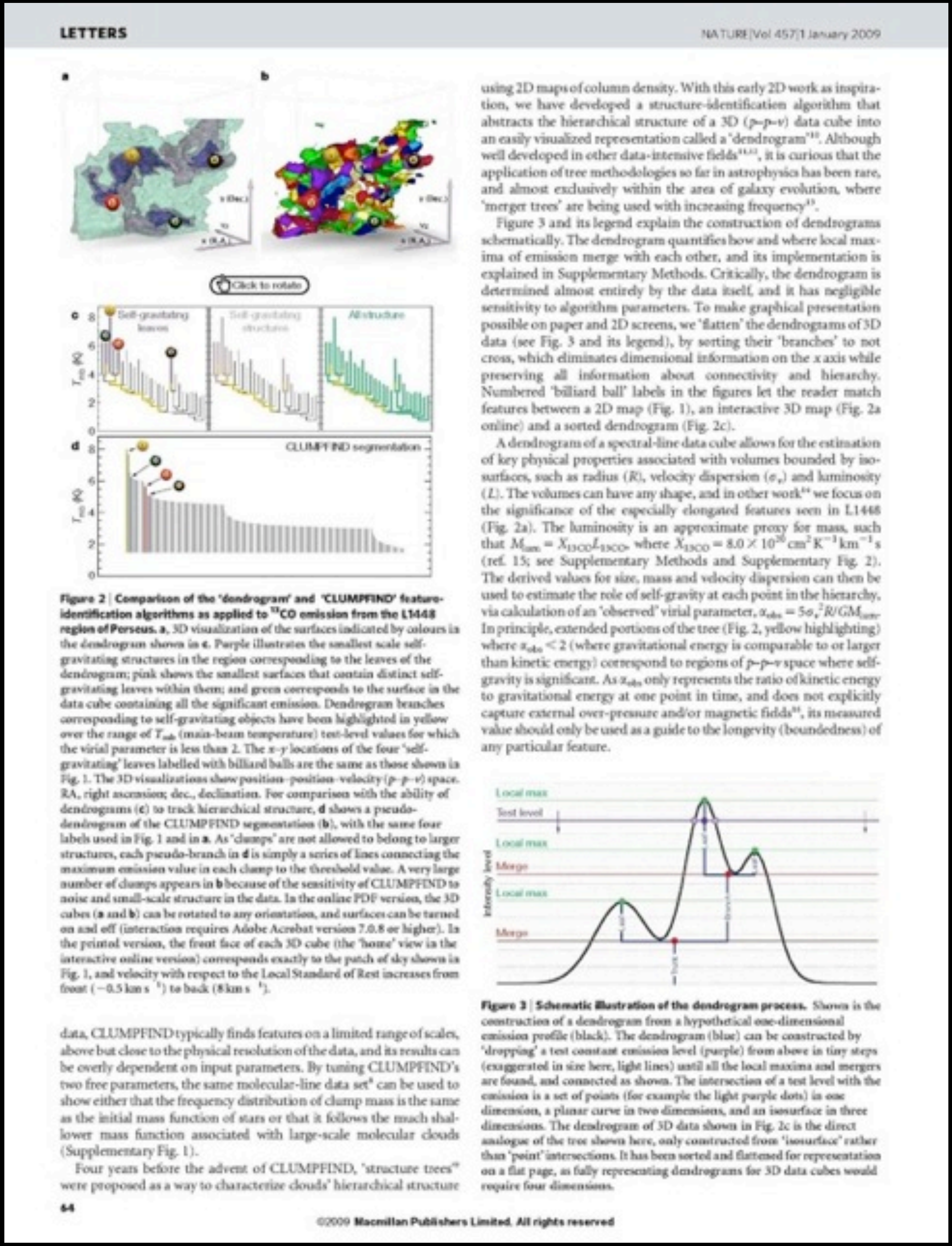

LETTERS NATURE|Vol 457|1 January 2009

Figure 2 | Comparison of the ‘dendrogram’ and ‘CLUMPFIND’ feature-identification algorithms as applied to ^{13}CO emission from the L1448 region of Perseus. a, 3D visualization of the surfaces indicated by colours in the dendrogram shown in **c**. Purple illustrates the smallest scale self-gravitating structures in the region corresponding to the leaves of the dendrogram; pink shows the smallest surfaces that contain distinct self-gravitating leaves within them; and green corresponds to the surface in the data cube containing all the significant emission. Dendrogram branches corresponding to self-gravitating objects have been highlighted in yellow over the range of T_{mb} (main-beam temperature) test-level values for which the virial parameter is less than 2. The x–y locations of the four ‘self-gravitating’ leaves labelled with billiard balls are the same as those shown in Fig. 1. The 3D visualizations show position–position–velocity (p–p–v) space. RA, right ascension; dec., declination. For comparison with the ability of dendrograms (**c**) to track hierarchical structure, **d** shows a pseudo-dendrogram of the CLUMPFIND segmentation (**b**), with the same four labels used in Fig. 1 and in **a**. As ‘clumps’ are not allowed to belong to larger structures, each pseudo-branch in **d** is simply a series of lines connecting the maximum emission value in each clump to the threshold value. A very large number of clumps appears in **b** because of the sensitivity of CLUMPFIND to noise and small-scale structure in the data. In the online PDF version, the 3D cubes (**a** and **b**) can be rotated to any orientation, and surfaces can be turned on and off (interaction requires Adobe Acrobat version 7.0.8 or higher). In the printed version, the front face of each 3D cube (the ‘home’ view in the interactive online version) corresponds exactly to the patch of sky shown in Fig. 1, and velocity with respect to the Local Standard of Rest increases from front (-0.5 km s^{-1}) to back (8 km s^{-1}).

data, CLUMPFIND typically finds features on a limited range of scales, above but close to the physical resolution of the data, and its results can be overly dependent on input parameters. By tuning CLUMPFIND’s two free parameters, the same molecular-line data set[8] can be used to show either that the frequency distribution of clump mass is the same as the initial mass function of stars or that it follows the much shallower mass function associated with large-scale molecular clouds (Supplementary Fig. 1).

Four years before the advent of CLUMPFIND, ‘structure trees’[9] were proposed as a way to characterize clouds’ hierarchical structure using 2D maps of column density. With this early 2D work as inspiration, we have developed a structure-identification algorithm that abstracts the hierarchical structure of a 3D (p–p–v) data cube into an easily visualized representation called a ‘dendrogram’[10]. Although well developed in other data-intensive fields[11,12], it is curious that the application of tree methodologies so far in astrophysics has been rare, and almost exclusively within the area of galaxy evolution, where ‘merger trees’ are being used with increasing frequency[13].

Figure 3 and its legend explain the construction of dendrograms schematically. The dendrogram quantifies how and where local maxima of emission merge with each other, and its implementation is explained in Supplementary Methods. Critically, the dendrogram is determined almost entirely by the data itself, and it has negligible sensitivity to algorithm parameters. To make graphical presentation possible on paper and 2D screens, we ‘flatten’ the dendrograms of 3D data (see Fig. 3 and its legend), by sorting their ‘branches’ to not cross, which eliminates dimensional information on the x axis while preserving all information about connectivity and hierarchy. Numbered ‘billiard ball’ labels in the figures let the reader match features between a 2D map (Fig. 1), an interactive 3D map (Fig. 2a online) and a sorted dendrogram (Fig. 2c).

A dendrogram of a spectral-line data cube allows for the estimation of key physical properties associated with volumes bounded by isosurfaces, such as radius (R), velocity dispersion (σ_v) and luminosity (L). The volumes can have any shape, and in other work[14] we focus on the significance of the especially elongated features seen in L1448 (Fig. 2a). The luminosity is an approximate proxy for mass, such that $M_{lum} = X_{13CO} L_{13CO}$, where $X_{13CO} = 8.0 \times 10^{20}$ cm^2 K^{-1} km^{-1} s (ref. 15; see Supplementary Methods and Supplementary Fig. 2). The derived values for size, mass and velocity dispersion can then be used to estimate the role of self-gravity at each point in the hierarchy, via calculation of an ‘observed’ virial parameter, $\alpha_{obs} = 5\sigma_v^2 R / G M_{lum}$. In principle, extended portions of the tree (Fig. 2, yellow highlighting) where $\alpha_{obs} < 2$ (where gravitational energy is comparable to or larger than kinetic energy) correspond to regions of p–p–v space where self-gravity is significant. As α_{obs} only represents the ratio of kinetic energy to gravitational energy at one point in time, and does not explicitly capture external over-pressure and/or magnetic fields[16], its measured value should only be used as a guide to the longevity (boundedness) of any particular feature.

Figure 3 | Schematic illustration of the dendrogram process. Shown is the construction of a dendrogram from a hypothetical one-dimensional emission profile (black). The dendrogram (blue) can be constructed by ‘dropping’ a test constant emission level (purple) from above in tiny steps (exaggerated in size here, light lines) until all the local maxima and mergers are found, and connected as shown. The intersection of a test level with the emission is a set of points (for example the light purple dots) in one dimension, a planar curve in two dimensions, and an isosurface in three dimensions. The dendrogram of 3D data shown in Fig. 2c is the direct analogue of the tree shown here, only constructed from ‘isosurface’ rather than ‘point’ intersections. It has been sorted and flattened for representation on a flat page, as fully representing dendrograms for 3D data cubes would require four dimensions.

64

Goodman et al. 2009; cf. Rosolowsky et al. 2008.

Taste-Testing Gravity(?)

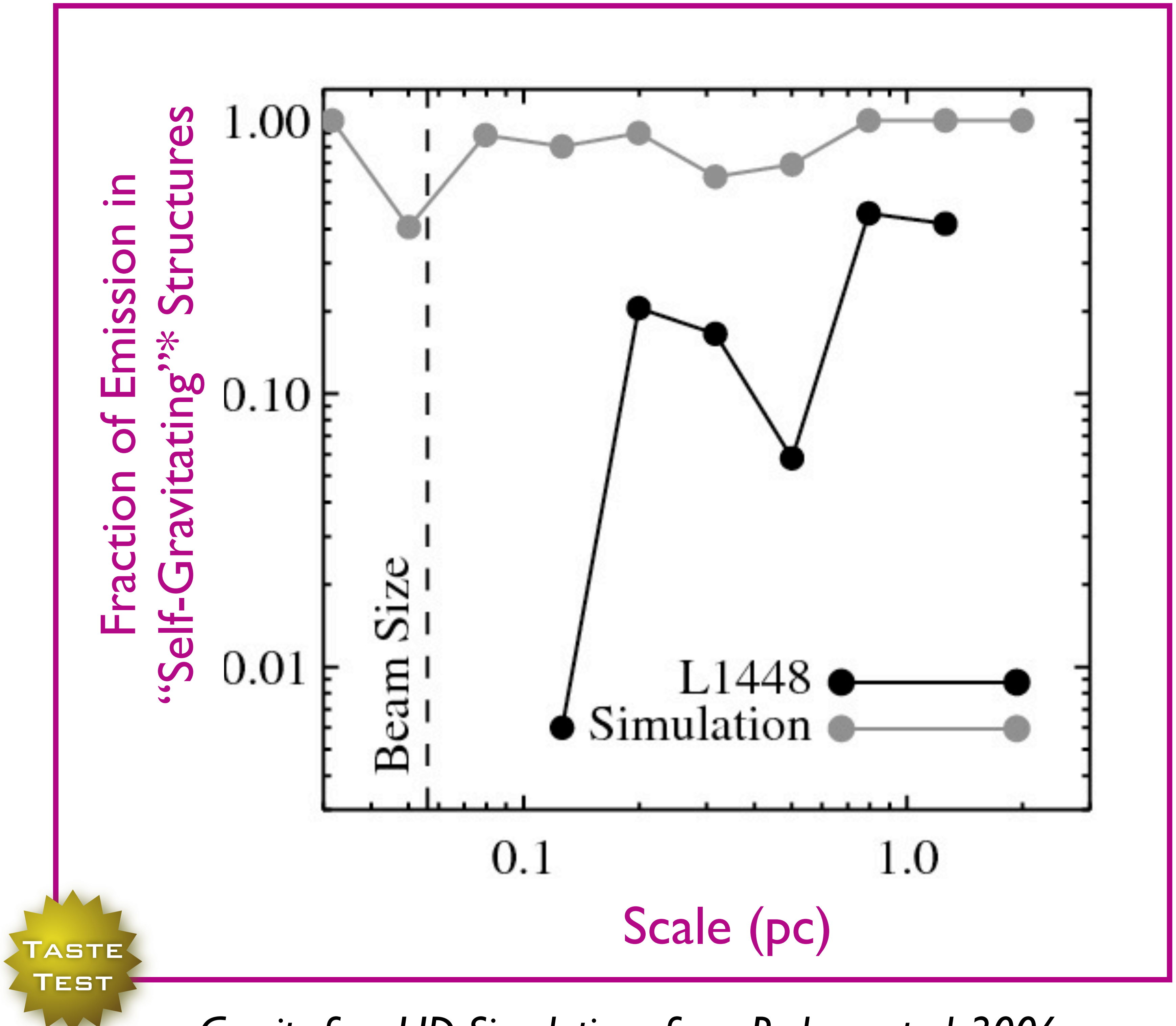

Gravity-free HD Simulations from Padoan et al. 2006;
L1448 analysis from Rosolowsky et al. 2008
both lines derived from ^{13}CO "observations"

Matching "Power Spectra" are not enough...

TASTE TEST

"Perseus-Matching"
Sample Simulation
from Padoan, Juvela, Kritsuk & Norman 2006
(Mach 6; Enzo; pure hydro)

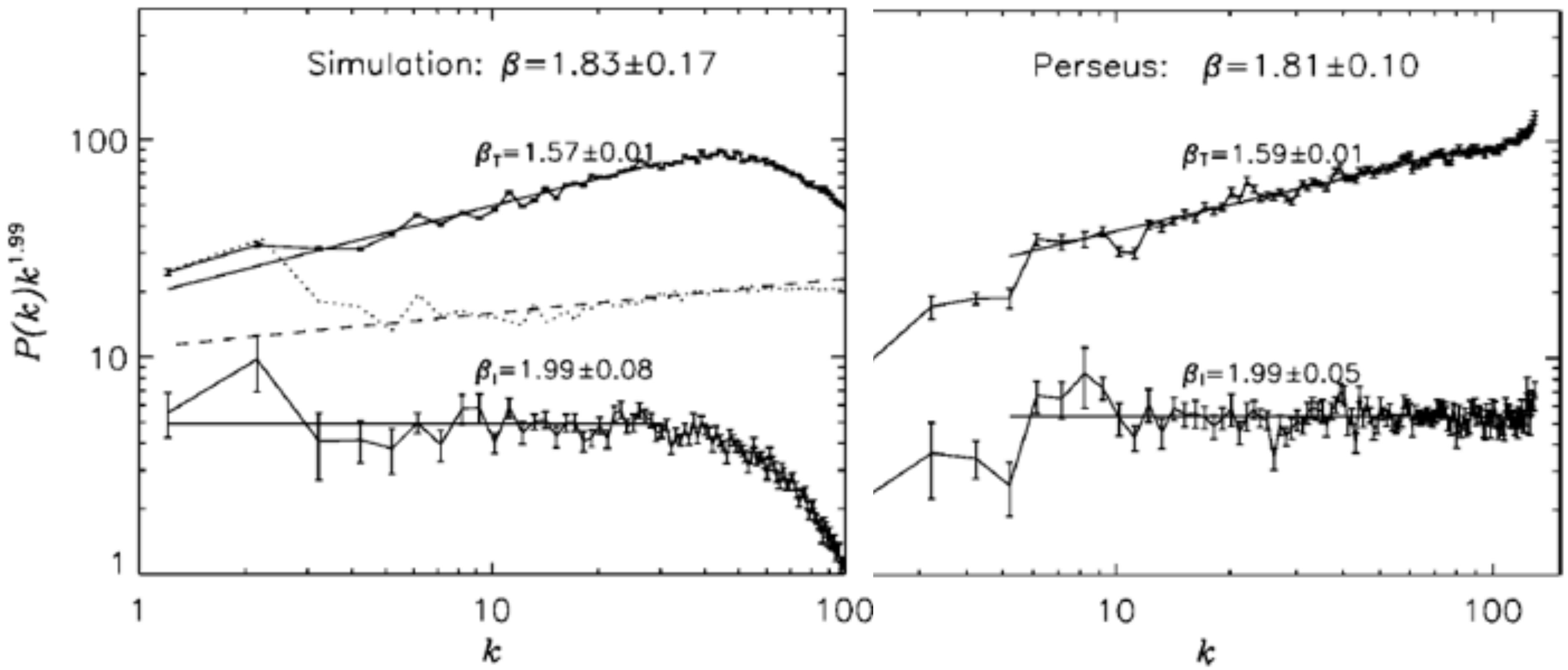

Note: Padoan et al. 2006 paper was intended to test the VCS method of Lazarian & Pogosyan 2000; cf. PCA methods of Brunt & Heyer 2002a,b

Caveats/Worries about *p-p-v* (bijection) ... and the virial parameter

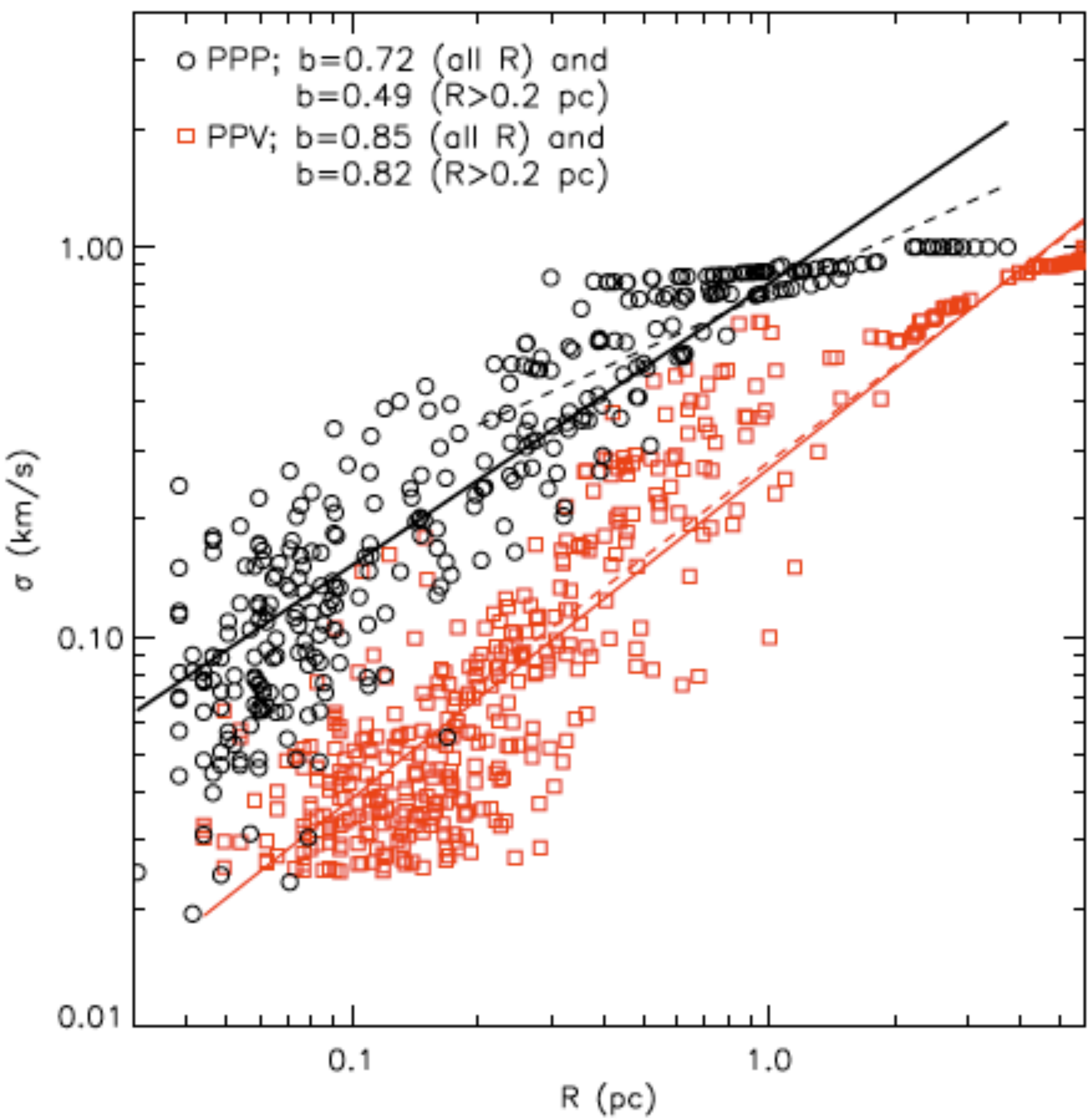

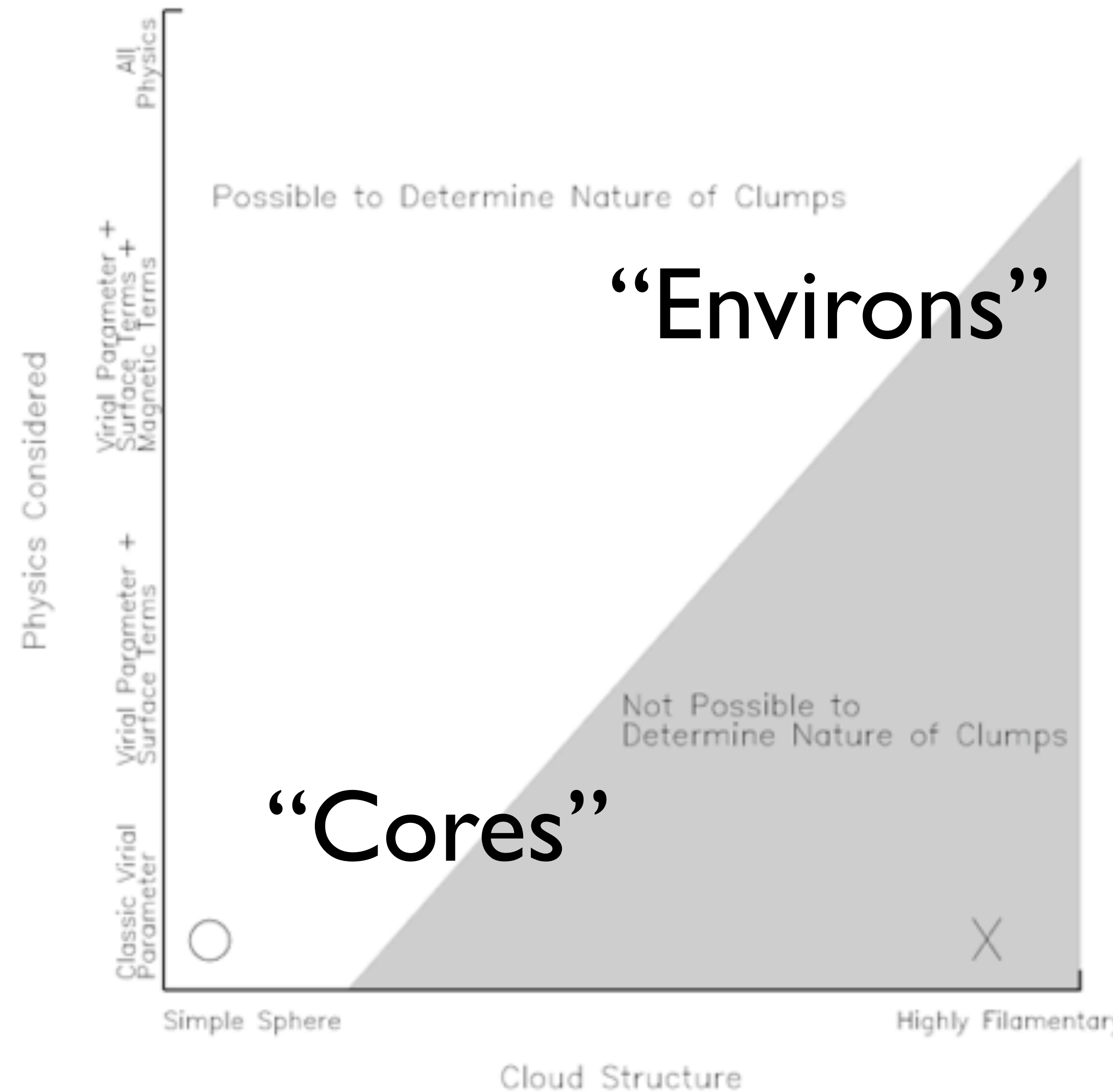

*from **Shetty**, Collins, Kauffmann, Goodman, Rosolowsky & M. Norman 2010;*
see also recent work of Dib et al., Ostriker et al., Ballesteros-Paredes et al., Myers, and Smith, Clark & Bonnell

Watermelons to Apples to Seeds?

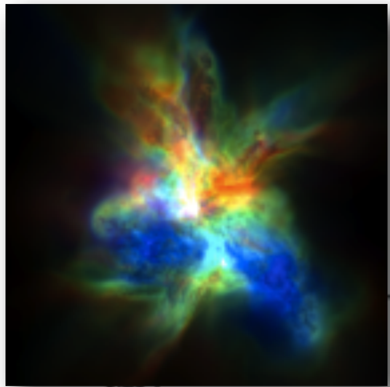

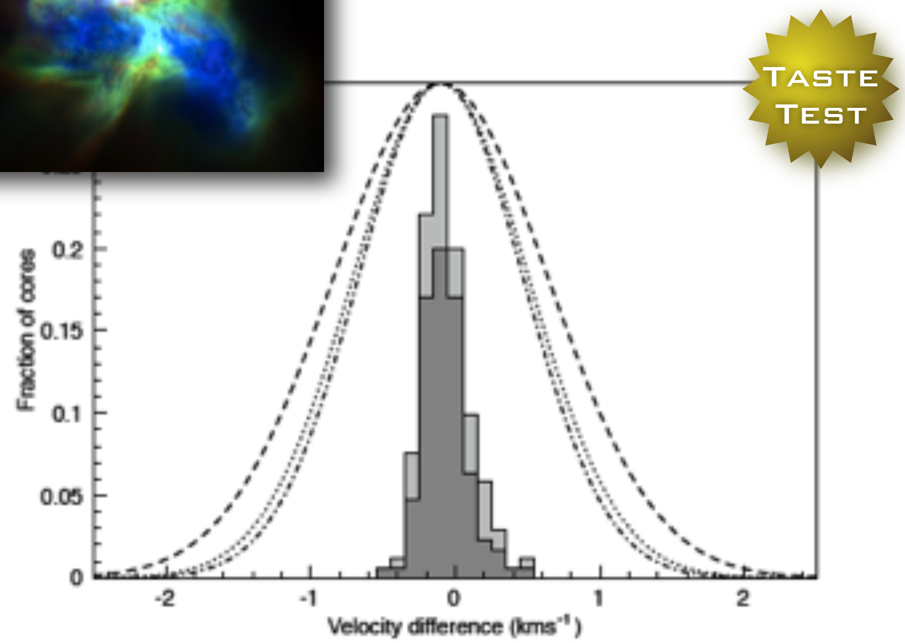

Figure 16. Histogram of velocity difference of all cores (combined starless and protostellar cores) identified at all time steps (light grey, $\sigma = 0.16$ km s^{-1}) and protostellar cores (dark grey, $\sigma = 0.18$ km s^{-1}). Also plotted are the velocity dispersions for N_2H^+ (dot, $\sigma = 0.861$ km s^{-1}), $C^{18}O$ (dot-dash, $\sigma = 0.808$ km s^{-1}), ^{13}CO (dash, $\sigma = 1.05$ km s^{-1}).

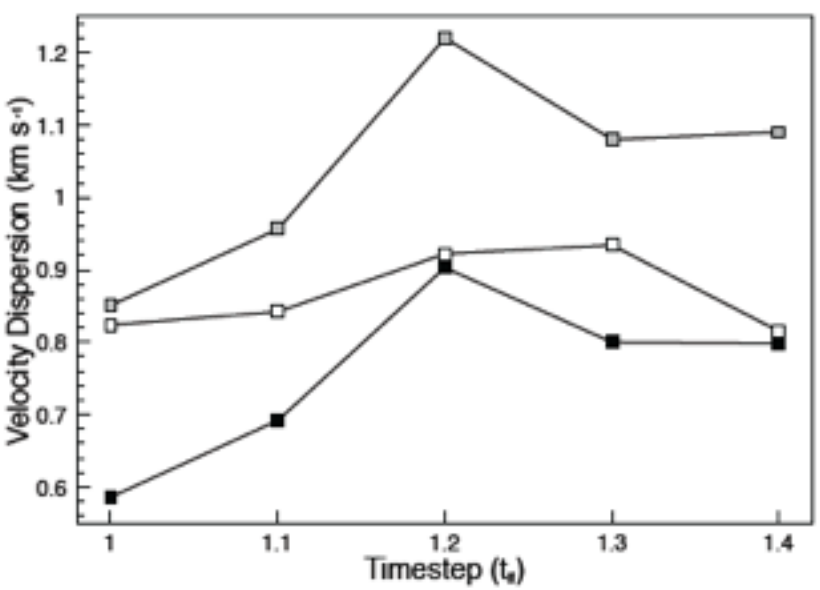

Rundle, Harries, Acreman & Bate 2010
cf. Ayliffe et al. 2007

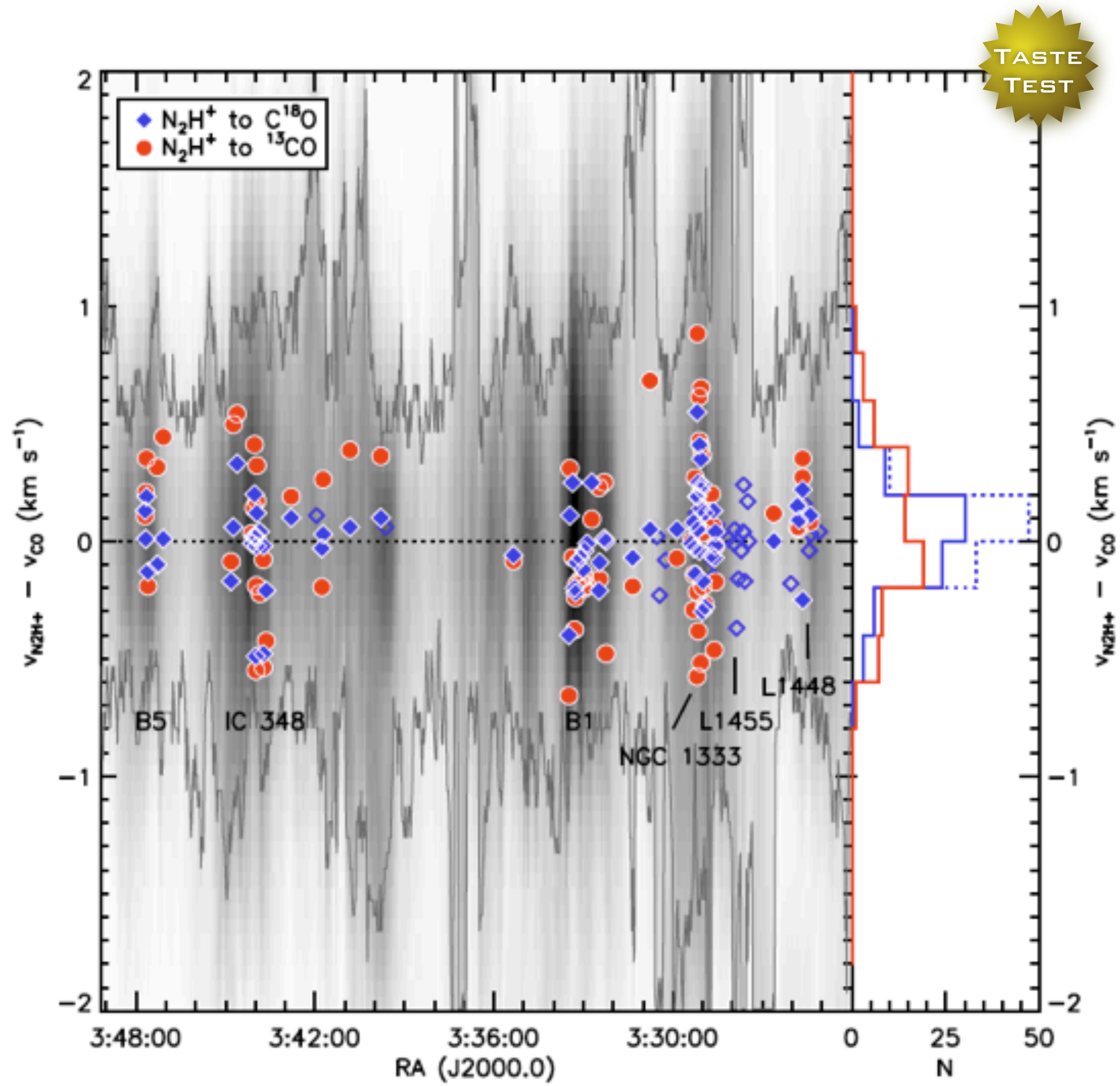

Kirk, Pineda, Johnstone & Goodman 2010;
see also Kirk, Johnstone & Basu 2009

Two Culinary Challenges from Jaime Pineda's Thesis!

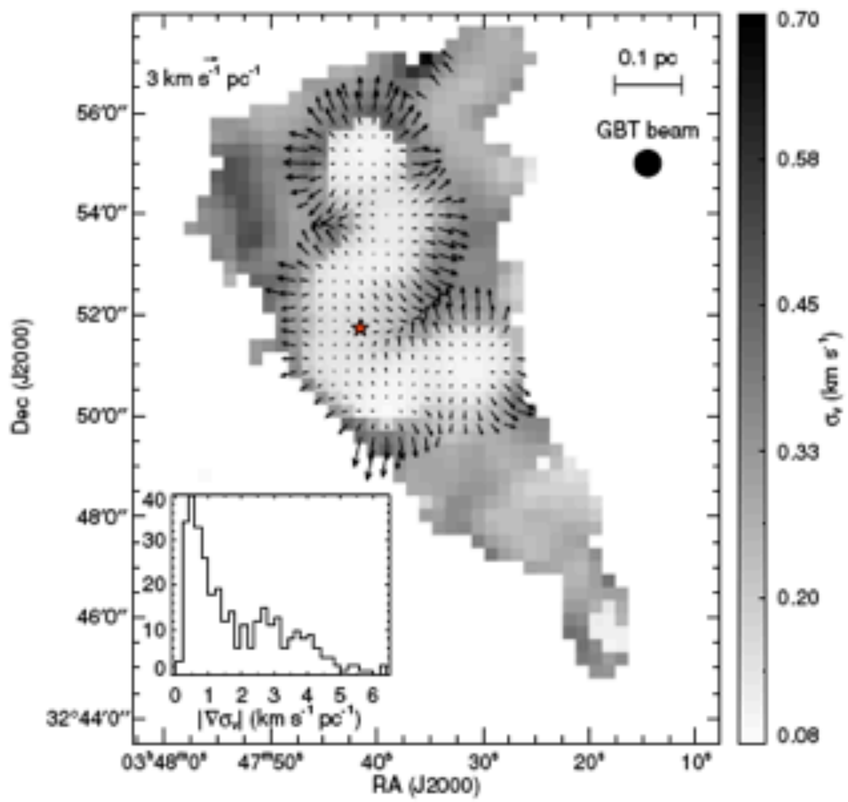

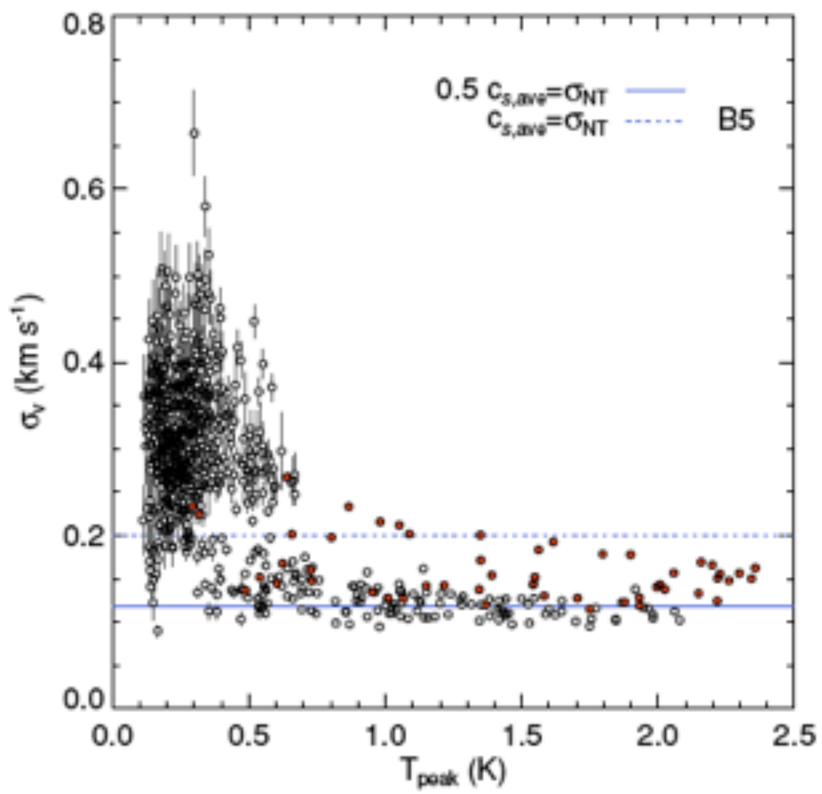

***Very** sharp transition to coherence in cores. (Chef Ostriker?)*

Pineda et al. 2010a

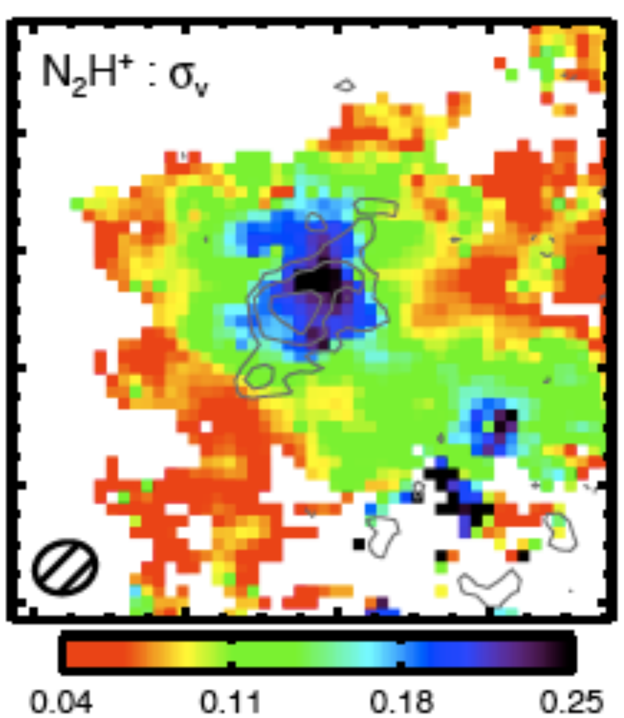

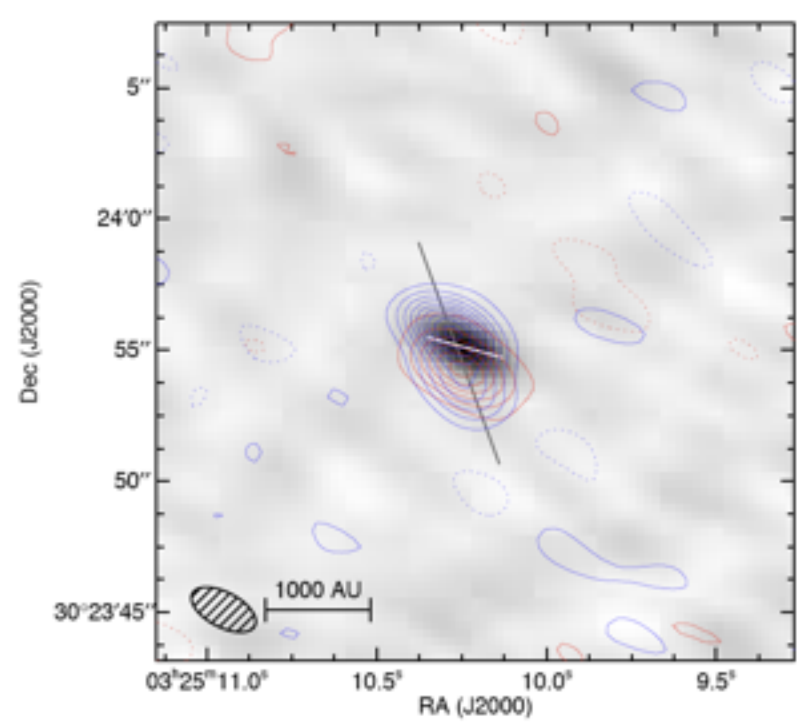

"First Core"
with an outflow
& no Spitzer source
cf. Chen, Arce et al. 2010
(Chef Machida?)

Pineda et al. 2010b

The New Chefs

Diner Beware?

"lognormals" from many non-turbulent "recipes"

(Andrea Urban's Poster)

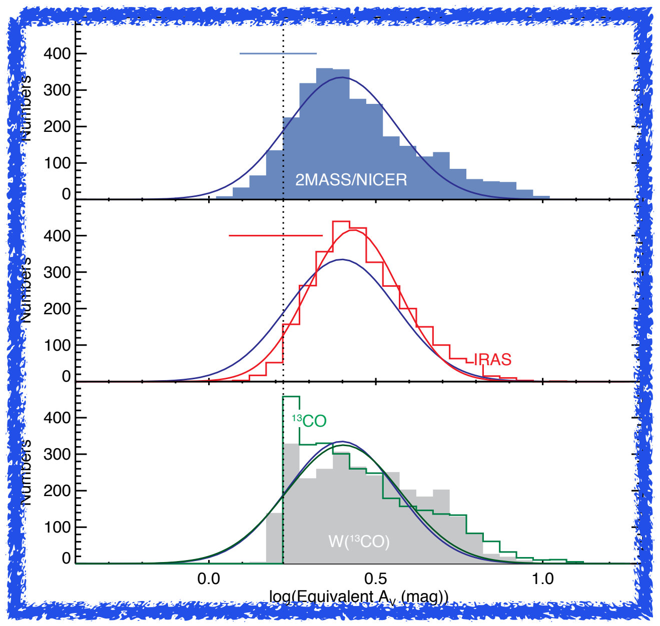

Analytic smooth density profile with *no* density perturbations.

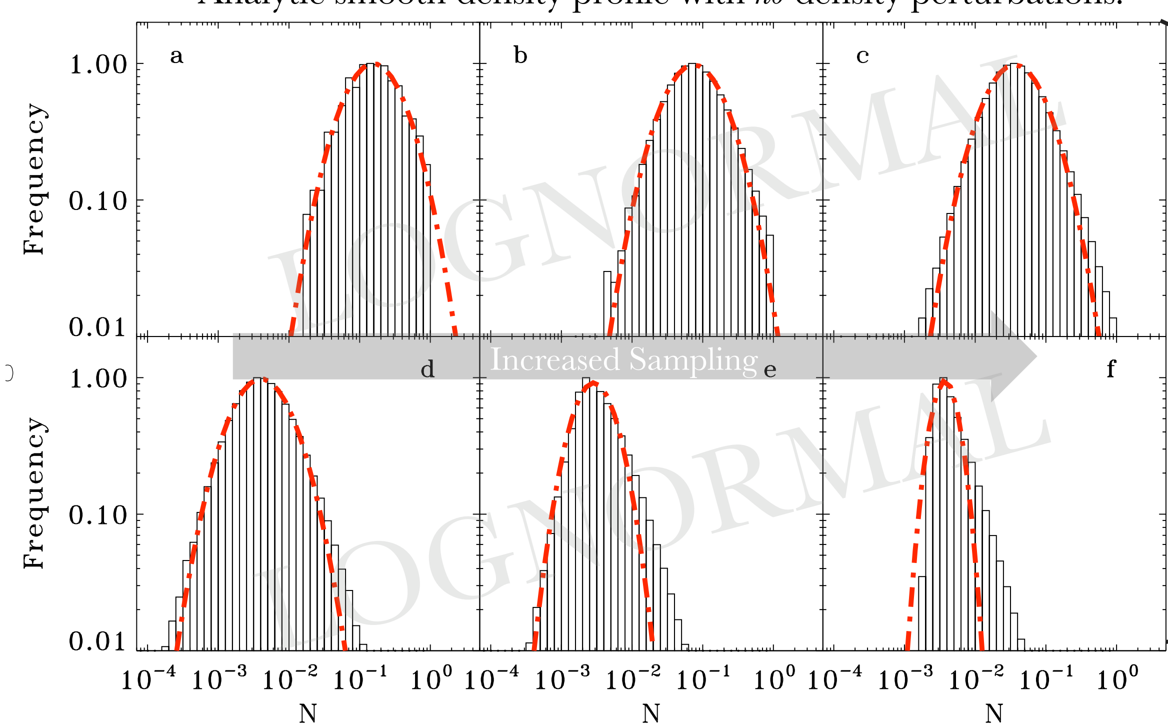

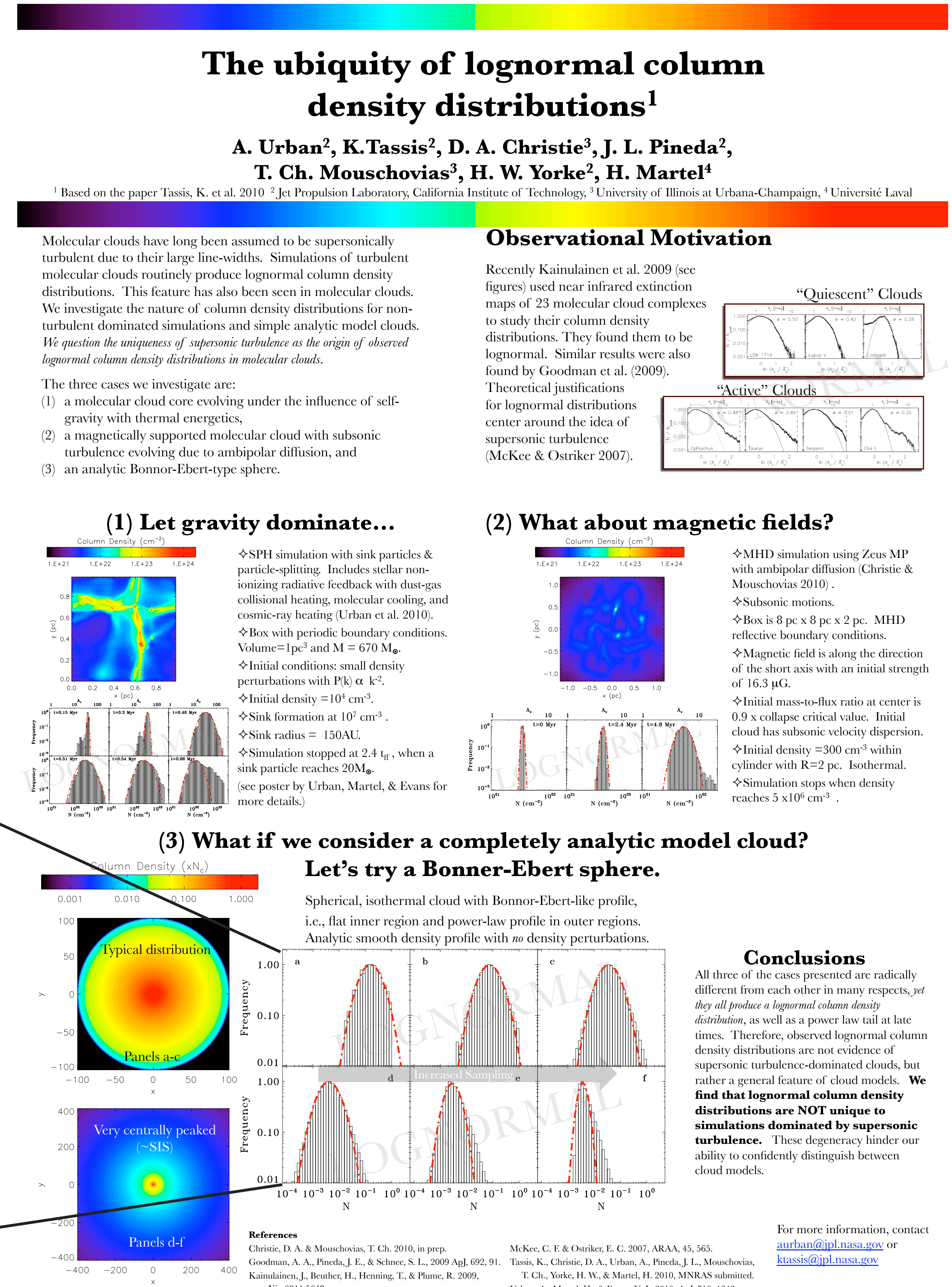

Column Density in Perseus, Measured 3 Ways

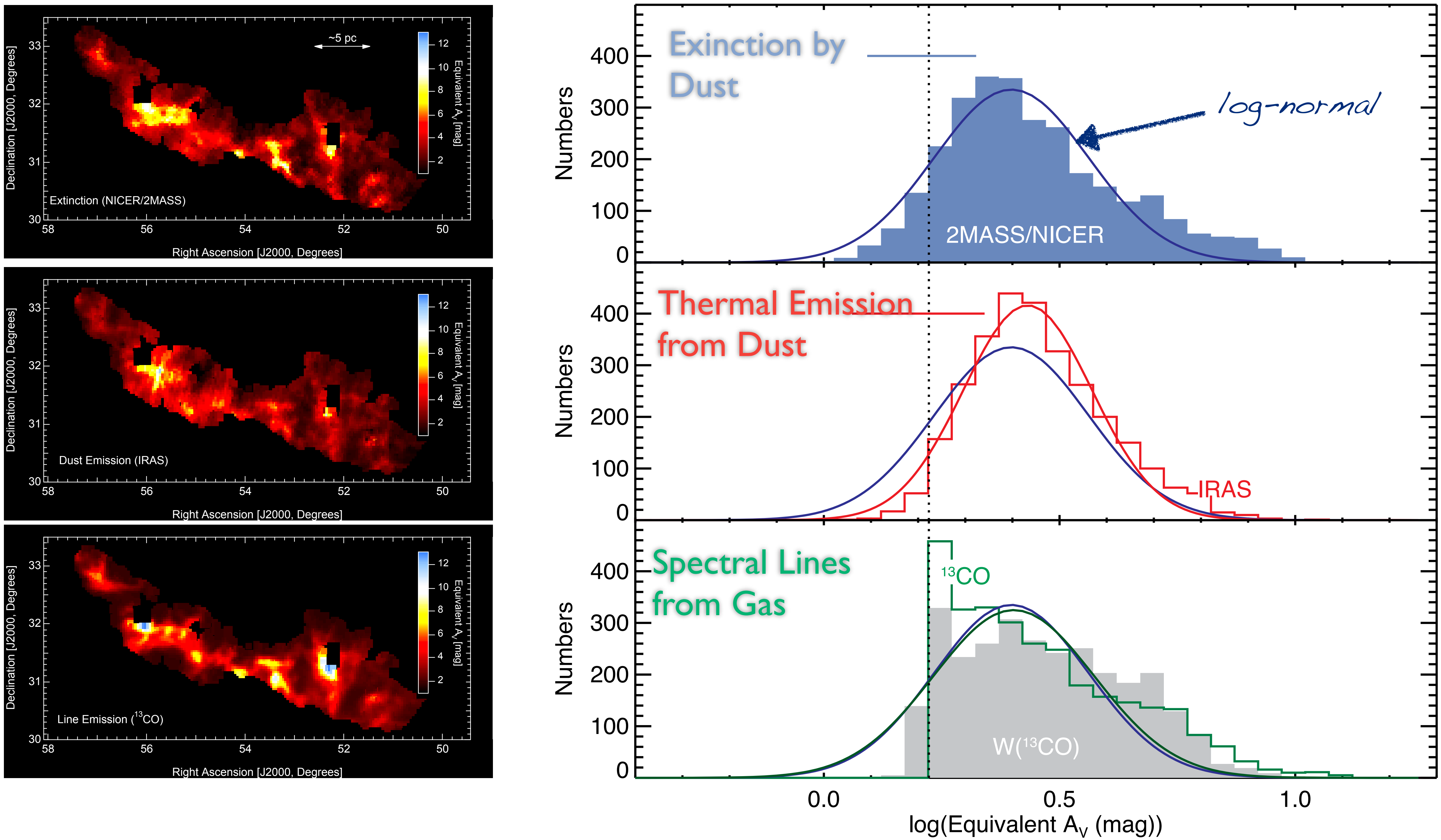

Goodman, Pineda & Schnee 2009, see also Pineda, Caselli & Goodman 2008